

Ultimate Loss Reserve Forecasting using Bidirectional LSTMs

by

Lahiru H. Somaratne¹

Supervised by Prof. Colin M. Ramsay

Abstract

This paper aims to demonstrate how deep learning (a subset of machine learning) can be used to forecast the ultimate losses of a sample group of Property and Casualty insurance companies. The paper initially explores the concept of loss development - how losses incurred by an insurance company mature across time. These losses then reach a final amount, known as the ultimate loss. The paper also looks at some already existing methods of forecasting the ultimate loss. The paper then introduces a novel method of forecasting losses, one which involves the use of deep learning neural networks. This new method uses Long Short Term Memory (LSTM) - an advanced form of a deep learning architecture which specializes in finding patterns in temporal data. The findings of this method are then compared to a currently existing Python package which can also be used to predict ultimate losses. The paper also goes to critique some shortcomings of the model that is presented.

Key words and phrases: loss reserves, machine learning, deep learning, LSTM

¹University of Nebraska-Lincoln, College of Business, Actuarial Science Program, Lincoln NE 68588-0490, USA. E-Mail: lahiru.somaratne@huskers.unl.edu

15 **1 Introduction**

16 **1.1 The life of a claim**

17 A claim is a policyholder's request for financial indemnification from an insurance
18 company after a loss causing event. When a claim is brought to the knowledge of
19 the insurance company with whom the claimant has an insurance policy, the claim
20 is said to have been reported. The time elapsed between the occurrence date of
21 the event producing the claim and the date which the claim is reported is called
22 the reporting delay (Amin et al., 2020). Once the claim has been reported to the
23 insurer, a claim file is opened, and the claim development process begins where
24 the insurer takes the necessary steps to process and settle the claim. Once the
25 claim is settled, i.e. the claim is not expected to develop any further, the claim
26 is then closed (Closed claims can be reopened if necessary). The time between
27 the date the claim is reported and the date when the claim is closed is called the
28 settlement delay (Amin et al., 2020). The settlement delay can be separated into
29 time periods, called lag periods. At the end of each lag period, we can observe
30 the state of the claim in terms of how much it has developed or changed over the
31 previous lag periods. Due to the settlement delay that is inherent in any claim
32 development process, the insurer at any time can have claims that are open and
33 not fully developed. The state of development correlates with how far back in time
34 the relevant claim was reported. The further back in time a claim was reported,
35 the longer time it has had to develop, which can cause the oldest claims to be fully
36 developed and closed.

37 To better manage its open claims, insurers often aggregate claims by the acci-
38 dent year (or the underwriting year), the development year, or the calendar year
39 (or the accounting year) (Radtke, 2016, 242). The variables used to measure aggre-
40 gate claims are cumulative paid losses, loss reserves, or incurred losses (Radtke,
41 2016, 243). The cumulative paid losses for a particular claim at some time k rep-
42 represents the total dollar amounts the insurer paid with regards to the claim up until
43 time k . The loss reserves for a particular claim at some time k represents the in-
44 surer's estimate of the size of the unpaid claim remaining at time k . The incurred
45 losses for a particular claim at some time k represents the insurer's estimate of
46 the size of the claim increment from time $k-1$ to time k . This paper focuses on
47 loss development of cumulative paid losses because cumulative paid losses tend

48 to be more stable in the loss development pattern. Specifically, cumulative losses
 49 almost always follow a monotonically increasing function over time, which makes
 50 predicting cumulative losses an easier task.

51 1.2 Data Representation for Loss Reserving

52 Data representation is an important aspect of loss reserving. Not only does it im-
 53 pact how the reader perceives data, the choice of how data is represented also
 54 impacts the choice of methods that can be used to develop loss data. The tradi-
 55 tional approach to representing loss reserving data is a loss development triangle
 56 where loss development data are grouped according to Accident Year (AY) and
 57 Development Year (DY). For example, suppose that we are looking at some hypo-
 58 theoretical loss data across 6 accident years (2000-2005), over 6 development years. If
 59 we regard the x-axis as development years and y-axis as accident years, we arrive
 60 at this tabular format shown in Table 1:

Table 1: Cumulative paid losses for accident years 2000–2005
 over absolute development years 2000–2005

Accident Year (AY)	Development Year (DY)					
	2000	2001	2002	2003	2004	2005
2000	100	120	150	160	188	192
2001		95	100	130	135	155
2002			111	106	110	130
2003				89	95	108
2004					109	115
2005						99

62 For AY 2004, the only observed losses are from development years 2004 and
 63 2005, because no data for AY 2004 exists for any time before 2004. Thus the ear-
 64 liest theoretical observation for any accident year exists on the leading diagonal,
 65 rendering any cells below this diagonal to be empty. A more efficient method of
 66 representing loss development data would be to change the development years
 67 from absolute to relative years. Development years defined in this manner refer to
 68 the n^{th} year period after year of the accident. For example, DY 1 refers to the time
 69 period between 1 and 2 years after the accident took place. Rearranging Table 1

70 in this fashion would yield Table 2. This is an example of a run-off table (Schmidt,
 71 2016, 248).

Table 2: Cumulative paid losses for accident years 2000–2005
 over relative development years 0–5

Accident Year (AY)	Development Year (DY)					
	0	1	2	3	4	5
2000	100	120	150	160	188	192
2001	95	100	130	135	155	
2002	111	106	110	130		
2003	89	95	108			
2004	109	115				
2005	99					

73 The counter diagonal gives the latest observable data (cumulative paid loss),
 74 for each accident year. The unobserved cumulative paid losses can be found below
 75 the counter diagonal (this data is currently empty). The final relative development
 76 period for each accident year gives the ultimate losses. These losses are matured
 77 losses which can be regarded as having reached full development. The objective
 78 of this paper is to predict these ultimate paid cumulative losses.

79 **1.3 Loss Reserving Methods**

80 Although there are many methods for estimating property/casualty loss reserves,
 81 there are a few methods that are most commonly used. The most well known
 82 method is the chain ladder method and there are many variations of the chain
 83 ladder method. Briefly, under the chain ladder method, the ratio of cumulative in-
 84 curred losses (called the loss development factor) is calculated for successive loss
 85 development years. Assuming we have a loss development triangle with at least
 86 some fully developed loss data, the average loss development factors across the
 87 accident years are used to calculate cumulative claim development factors, which
 88 are then used to project ultimate loss. The loss reserve is the difference between
 89 the projected ultimate loss and the paid incurred loss. In general, loss reserv-
 90 ing methods can broadly be classified as being based on a parametric model or a
 91 non-parametric model. Traditionally, parametric models have been used due to

92 ease of interpretation and calculation. Models such as the over-dispersed Pois-
93 son, negative binomial, lognormal, and gamma models have been shown to be
94 capable of replicating the chain ladder based reserving methods (England & Ver-
95 rral, 11). These models are centered around estimating some parameters such
96 as the means and the variances, either by accident year or loss development pe-
97 riod, or both. Doing so condenses the number of parameters used by the model
98 and helps in identifying the ‘ingredients’ that went towards estimating the losses.
99 However, the assumptions needed in the process of constructing parametric mod-
100 els can limit the predictive power of the model. Particularly in the case where the
101 underlying factors which drive the dynamic relationships between data is not well
102 understood, non-parametric models can outperform parametric models (Mills &
103 Markellos, 2008, 224).

104 A common feature of established loss reserving methods is their reliance on
105 the existence of a sufficiently long loss run-off triangle. Ramsay (2007, 462) de-
106 veloped a non-parametric loss reserving method/process to assist them with their
107 “best guess” in the early years of development and with loss reserving in gen-
108 eral. Ramsay’s method is fundamentally different from previous loss reserving
109 methods. Given that losses are settled in n years, Ramsay’s method assumes the
110 evolution of the incremental incurred loss over development years is the result of
111 a random split of the ultimate loss for that accident year into n separate pieces of
112 losses, which are then ordered from largest to smallest. The largest incremental
113 loss is observed in the first development year, the second largest incremental loss
114 is observed in the second development year, etc, so that the smallest incremen-
115 tal loss is observed in the last development year. Ramsay’s approach requires no
116 prior knowledge of the distribution of the ultimate loss or of the actual cumulative
117 incurred loss. In addition, it uses little or no loss development data.

118 **Our Objective:** To use deep learning to provide a loss reserving tool for actuar-
119 ies to use loss development data to produce more efficient and accurate estimates
120 of property and casualty loss reserves. Although we will use order statistics, our
121 approach is different from Ramsay (2007).

122 2 Machine Learning and Deep Learning

123 In order to properly understand what deep learning is, we must briefly visit what
124 machine learning is, since the former is a subset of the later. Central to the debate

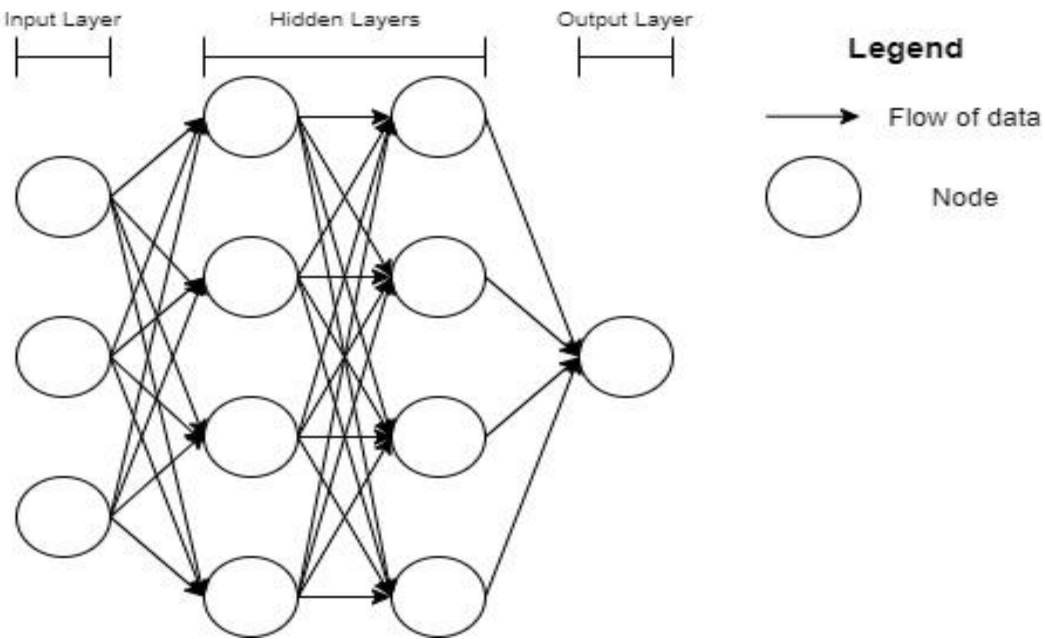
125 of what machine learning is, is the question, “Rather than programmers crafting
126 data-processing rules by hand, could a computer automatically learn these rules
127 by looking at data?”. A distinct advantage that machine learning has over classical
128 statistics is the ability of machine learning models to handle data of a large volume,
129 which can sometimes be a challenge to classical statistical methods (Chollet, 2018).

130 Machine Learning can be broadly divided into three areas: supervised learning,
131 unsupervised learning, and reinforcement learning. In supervised learning, data
132 fed into a machine learning algorithm are divided into dependent and indepen-
133 dent variables. It is called supervised learning because the dependent variables
134 act as a guide, in helping identify the patterns that exist in the data. The unsuper-
135 vised learning process has no dependent variable to measure the learning process
136 against. Instead, the features of data are observed and similarities between data
137 points are determined (Hastie et al., 2017). The last type of learning is reinforce-
138 ment learning; the process of using a reward structure to make the algorithm learn
139 the best course of action under a given set of circumstances (Sutton & Barto, 2018).

140 Supervised learning can be further broken down into problems that involve re-
141 gression or problems that involve classification, where the objective of regression
142 problems is to predict some value such as a reserve forecast and the objective of
143 classification problems is to identify if an outcome belongs to certain class, such
144 as if a loss ratio will exceed a certain threshold. Since many problems that actu-
145 aries deal with involve some level of financial prediction, most actuarial problems
146 can be viewed as regression problems. Expressing actuarial problems as regres-
147 sion problems makes them suitable to be solved using machine learning (Richman,
148 2020, 230-258).

149 Deep learning is a subset of machine learning which learns increasingly more
150 meaningful representations of data in a more hierarchical fashion. You could look
151 at other forms of machine learning as ‘shallow learning’, since they do not use as
152 many hierarchical layers to learn about meaningful patterns in the data that they
153 receive (Chollet, 2018). The key advantage of learning patterns in a hierarchical
154 fashion is that at various levels of abstraction, various patterns can be discovered.
155 It is easier to discover more granular patterns present in data this way. A typical
156 implementation of a deep learning model is via a neural network, as shown in
157 Figure 1. There are many different flavors of neural networks, each being unique in
158 its own way. For the purpose of simple illustration of the concept, we will present
159 a figure of a neural network, which utilizes a fully connected feed-forward neural

160 network structure.

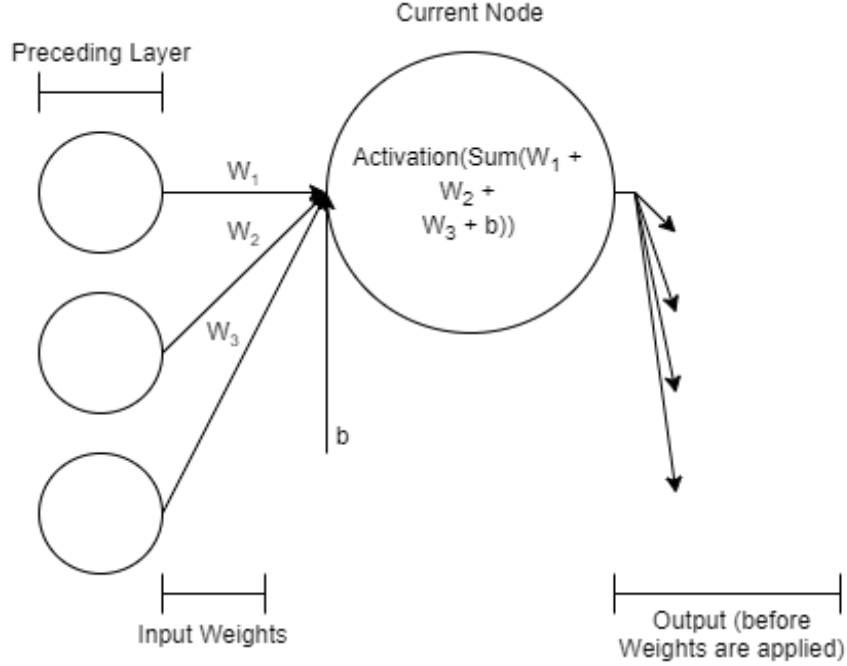


161

162

Figure 1: Fully Connected Feedforward Neural Network

163 In the example of a neural network given in Figure 1, each node receives input
164 from all nodes of the previous layer. This network has an input layer I , that takes
165 in 3 inputs, $I \in \mathbb{R}^3$. Similarly, the output layer O , utilizes 1 node to output 1
166 value, $O \in \mathbb{R}^1$. Barring the input layer, each node of each layer implements a linear
167 regression function. Figure 2 shows the workings of a node up close.



168

169

Figure 2: Functioning of a node

170 As mentioned before, each node (other than the input nodes) receives output from
 171 the preceding layer of nodes, as an input into it (Zhang et al., 2021). The inputs
 172 are each weighted differently. Therefore, we can represent the weighted inputs
 173 into the node as $w_i\beta_i$, where w_i represents the i^{th} weight, β_i represents the i^{th}
 174 input into the node, for $i = 1, 2, \dots, n$ and n represents the i^{th} input. These inputs
 175 also contain a bias term b . The data that is aggregated inside the node this way, is
 176 finally fed through an activation function to get the final output:

$$\text{node output} = f\left(b + \sum_{i=1}^n w_i\beta_i\right) \quad (1)$$

177 where $f(x)$ is an activation function for $x \in \mathbb{R}$. A typical activation function used
 178 would be the “sigmoid” activation function ¹:

$$f(x) = \frac{1}{1 + e^{-x}} \quad (2)$$

179 where $x \in \mathbb{R}$. As mentioned before, there are many flavors of neural networks
 180 and the type of network that will be the focus of this paper is a supervised neu-

¹This is also the inverse logit function.

181 ral network, where data is fed in the form of dependent variables (features) and
 182 independent variables (labels).

Dependent Variable	Independent Variables		
Label	Feature 1	...	Feature m
value ₁	value _{1,1}	...	value _{1,n}
...
value _n	value _{n,1}	...	value _{n,m}

183
 184 Figure 3: The general structure of a dataset of with n features and m rows

185 Features are fed into the input layer and passed forward through the network,
 186 where at the end of the network (the output layer), predictions are made. These
 187 predictions are then evaluated by a loss function, which aims to calculate the error
 188 of the predictions. Typically, the mean squared error function is used (Alzubaidi
 189 et al., 2021, 20):

$$L(\hat{y}, y) = \frac{1}{2N} \sum_{i=0}^N (\hat{y} - y) \quad (3)$$

190 where \hat{y} is the predicted output and y is the actual output. Optimizing the loss
 191 function means that the predicted output of the neural network needs to be as
 192 close as possible to the actual output of the data set. This process of optimizing
 193 is called training the network. As mentioned earlier, each neuron of each layer
 194 of the neural network has its own respective weights that regulate the strength
 195 of incoming signals from the preceding layers and biases. Therefore, we need
 196 to change these weights and biases through a process known as backpropagation,
 197 where all of the network's weights and biases are optimized, with respect to a given
 198 loss function (Zhang et al., 2021). The goal here is to minimize the given loss and
 199 in turn find the weight and bias settings that enable this said minimization:

$$w', \beta' = \arg \min_{w, \beta} L(\hat{y}, y) \quad (4)$$

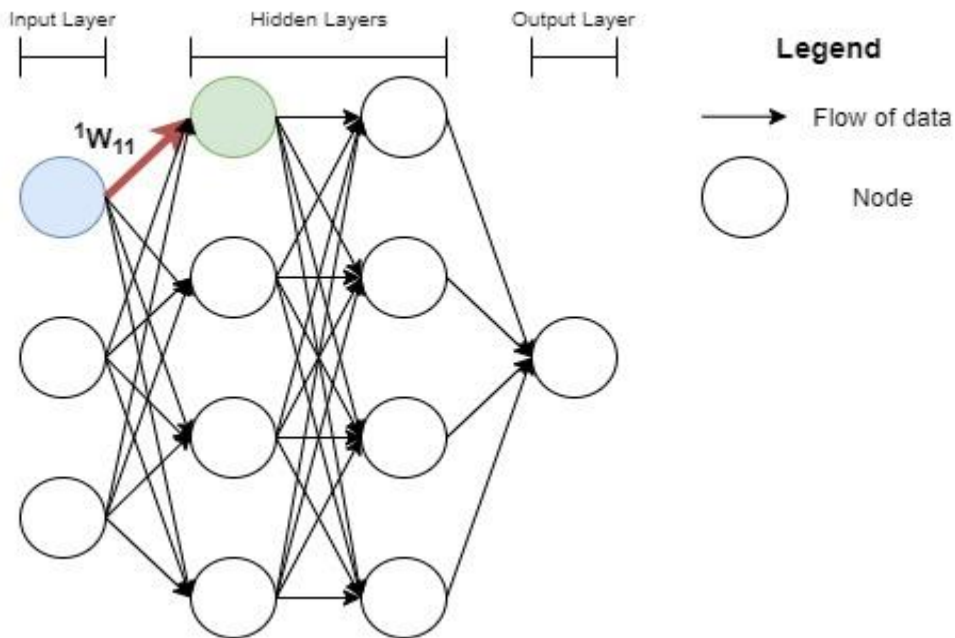
200 where w' and β' are network optimized weights and biases. Through backprop-
 201 agation and using the multidimensional gradient descent method, we are able to
 202 iteratively adjust the weights and biases of the network, taking into consideration

203 the sensitivity of each weight and bias, in relation to the loss function. The goal
 204 is to optimize weights in proportion to the impact that their change has on mini-
 205 mizing the loss . We can represent the optimization task on a given weight as the
 206 following partial derivative:

$$\Delta^{(k)}w_{ij} = -\eta \frac{\partial L}{\partial^{(k)}w_{ij}} \quad (5)$$

207 where $\Delta^{(k)}w_{ij}$ represents the change in given weight, k represents the layer which
 208 the weight belongs to, i is the destination node (the node which receives the weight),
 209 j is the origin node (the node which outputs the weight), and η is the learning rate
 210 (a tunable hyperparameter of the model). Thus the newly optimized weight can
 211 be represented as:

$${}^{(k)}w'_{ij} = {}^{(k)}w_{ij} + \Delta^{(k)}w_{ij} \quad (6)$$



212

Figure 4: A demonstration of a weight

213

214 We can represent the optimization process to include all weights and biases as:

$$\Delta \mathbf{W} = (\Delta^{(1)} \mathbf{w}, \Delta^{(2)} \mathbf{w}, \dots, \Delta^{(p)} \mathbf{w}) \quad (7)$$

where $\Delta\mathbf{W}$ is a $(m \times n \times p)$ 3D matrix composed of individual matrices containing the changes in weights and biases, for each layer of the network, and, for $r = 1, 2, \dots, p$,

$$\Delta^{(r)} \mathbf{w} = \begin{bmatrix} \Delta^{(r)} w_{11} & \Delta^{(r)} w_{12} & \cdots & \Delta^{(r)} w_{1n} \\ \Delta^{(r)} w_{21} & \Delta^{(r)} w_{22} & \cdots & \Delta^{(r)} w_{2n} \\ \vdots & \vdots & \cdots & \vdots \\ \Delta^{(r)} w_{m1} & \Delta^{(r)} w_{m2} & \cdots & \Delta^{(r)} w_{mn} \end{bmatrix} \quad (8)$$

215 and p represents the maximum number of layers in the network. For simplicity,
 216 we assume that the number of nodes for each layer is fixed, and therefore the
 217 maximum number of origin nodes and maximum number of destination nodes
 218 are the same for any particular layer. Therefore at each iteration, a new 3D matrix
 219 \mathbf{W}' is created:

$$\mathbf{W}' = \mathbf{W} + \Delta\mathbf{W} \quad (9)$$

220 where

$$\mathbf{W} = ({}^1 \mathbf{w}, {}^2 \mathbf{w}, \dots, {}^p \mathbf{w}) \quad (10)$$

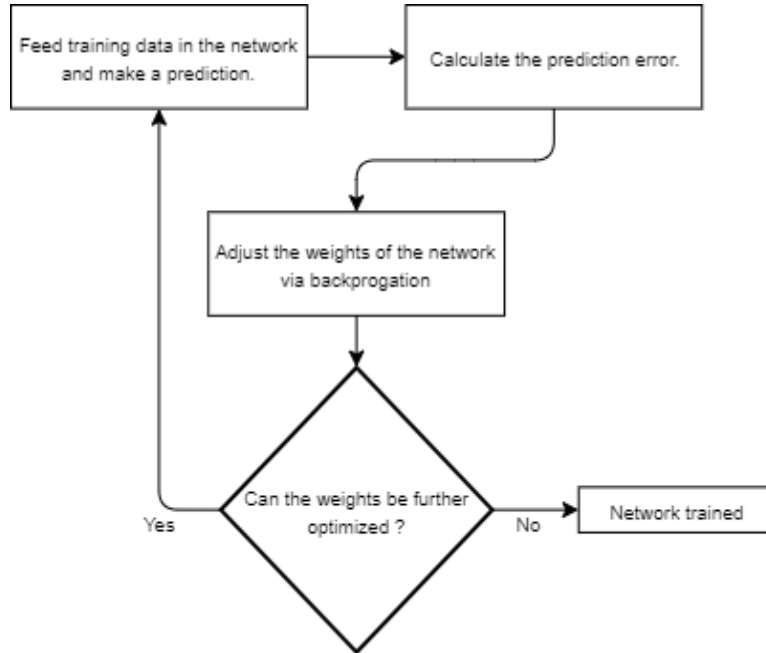
$$\mathbf{W}' = ({}^1 \mathbf{w}', {}^2 \mathbf{w}', \dots, {}^p \mathbf{w}') \quad (11)$$

and, for $r = 1, 2, \dots, p$,

$${}^{(r)} \mathbf{w} = \begin{bmatrix} {}^{(r)} w_{11} & {}^{(r)} w_{12} & \cdots & {}^{(r)} w_{1n} \\ {}^{(r)} w_{21} & {}^{(r)} w_{22} & \cdots & {}^{(r)} w_{2n} \\ \vdots & \vdots & \cdots & \vdots \\ {}^{(r)} w_{m1} & {}^{(r)} w_{m2} & \cdots & {}^{(r)} w_{mn} \end{bmatrix} \quad (12)$$

$${}^{(r)} \mathbf{w}' = \begin{bmatrix} {}^{(r)} w'_{11} & {}^{(r)} w'_{12} & \cdots & {}^{(r)} w'_{1n} \\ {}^{(r)} w'_{21} & {}^{(r)} w'_{22} & \cdots & {}^{(r)} w'_{2n} \\ \vdots & \vdots & \cdots & \vdots \\ {}^{(r)} w'_{m1} & {}^{(r)} w'_{m2} & \cdots & {}^{(r)} w'_{mn} \end{bmatrix} \quad (13)$$

221 where \mathbf{W} and \mathbf{W}' represent the 3D matrix of optimized weights and biases from
 222 the last iteration of the network optimization, and the 3D matrix of the newly
 223 optimized weights and biases, respectively. The weights and biases are adjusted,
 224 until the weights of the $\Delta\mathbf{W}$ matrix cause the training loss to begin increasing,
 225 instead of decreasing. This can be represented as shown in Figure 5:



226

227

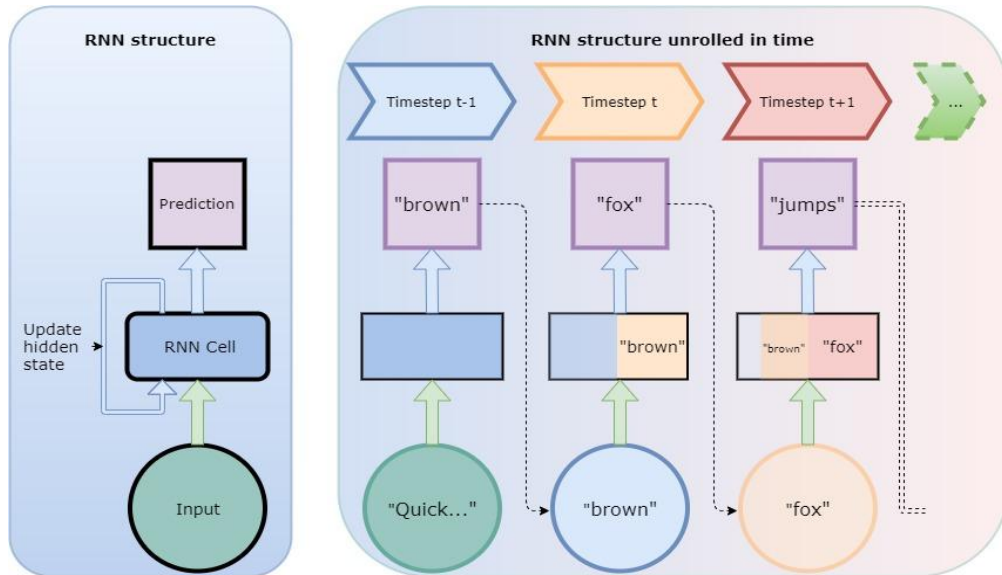
Figure 5: Neural network training process

228 3 Recurrent Neural Networks (RNNs)

229 As is evident by the introduction, loss development has a strong temporal compo-
 230 nent. Therefore, any deep learning model that is used to make loss development
 231 predictions needs to take this aspect of the data into account. For this reason,
 232 recurrent neural networks are a worthy choice to consider. The basic premise of
 233 these types of networks is the reliance of a past sequence of data to make a pre-
 234 diction. This can be represented as follows (Zhang et al., 2021): the conditional
 235 probability of observing x at time t (i.e., x_t), given previous observations at times 1,
 236 2, ..., $t - 1$ can be written as $\Pr(x_t|x_{t-1}, x_{t-2}, \dots, x_1)$. As it is generally prohibitively
 237 costly to store all information of a given sequence in memory, we therefore can
 238 retain the partial information given a certain subset of this sequence. This partial
 239 information subset can be identified as the hidden state, h_{t-1} . This leads to the
 240 conditional probability given the partial information as $\Pr(x_t|h_{t-1})$. The hidden
 241 state itself can be represented recursively as:

$$h_{t-1} = f(x_{t-1}|h_{t-2}) \tag{14}$$

242 where x_{t-1} is the observation at time $t - 1$ and h_{t-2} is the hidden state at time $t - 2$.
 243 In comparison to the node described before, a node of a RNN can be “unrolled”
 244 in time due to it having this hidden state. An intuitive illustration of how an
 245 RNN processes sequential data by remembering input from previous timesteps is
 246 depicted in Figure 6:



247 The sentence : "Quick brown fox jumps over the lazy dog."

248 Figure 6: How an RNN processes sequential data

249 As Figure 6 illustrates with the sentence “Quick brown fox jumps over the lazy
 250 dog,” at each time step, information from previous timesteps is used to predict
 251 the output at that time step. Note that the hidden state can only contain a finite
 252 amount of information and therefore tends to hold past information only within
 253 a certain time frame. Mathematically speaking, the introduction of hidden states
 254 now implies that there are more weights and biases to optimize. If we visualize
 255 the weights as matrices - for feedforward neural networks, we only have matrices
 256 with weights relating to the current time, t . With a hidden state, each weight will
 257 now have a hidden state version of it.

258 We can represent the flow of data of RNN in matrix notation in the following
 259 manner:

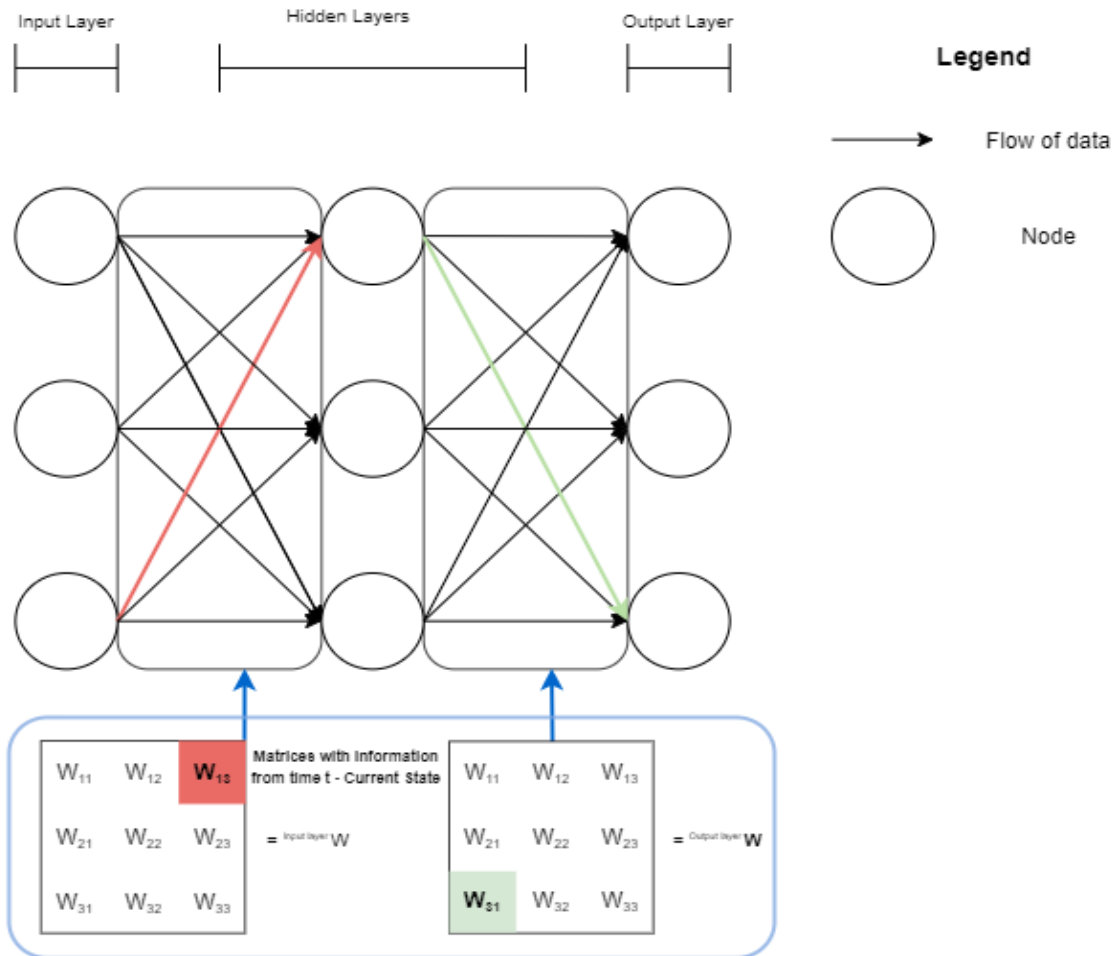
$$\mathbf{H}_t = \alpha(\mathbf{X}_t \mathbf{W} + \mathbf{H}_{t-1} \mathbf{W}_h) \tag{15}$$

260 where \mathbf{H}_t is the output vector of the hidden layer at time t , \mathbf{X}_t is the input vector at

261 time t , \mathbf{H}_{t-1} is the output vector of the hidden layer from time step $t - 1$ (also the
 262 hidden state at time t), \mathbf{W} is the weight matrix, of which the first layer is multiplied
 263 by \mathbf{X}_t . \mathbf{W}_h is the weight matrix of the hidden layers, of which the first layer is
 264 multiplied by \mathbf{H}_{t-1} , which is the same matrix discussed in Section 5, and α is the
 265 symbol of the activation function used in the respective layer. As \mathbf{W} and \mathbf{W}_h are
 266 composed of matrices \mathbf{W}^r and \mathbf{W}_h^r , respectively, where r refers to a layer of the
 267 neural network and p is the maximum number of hidden layers in the network),
 268 equation 15 can also be written as:

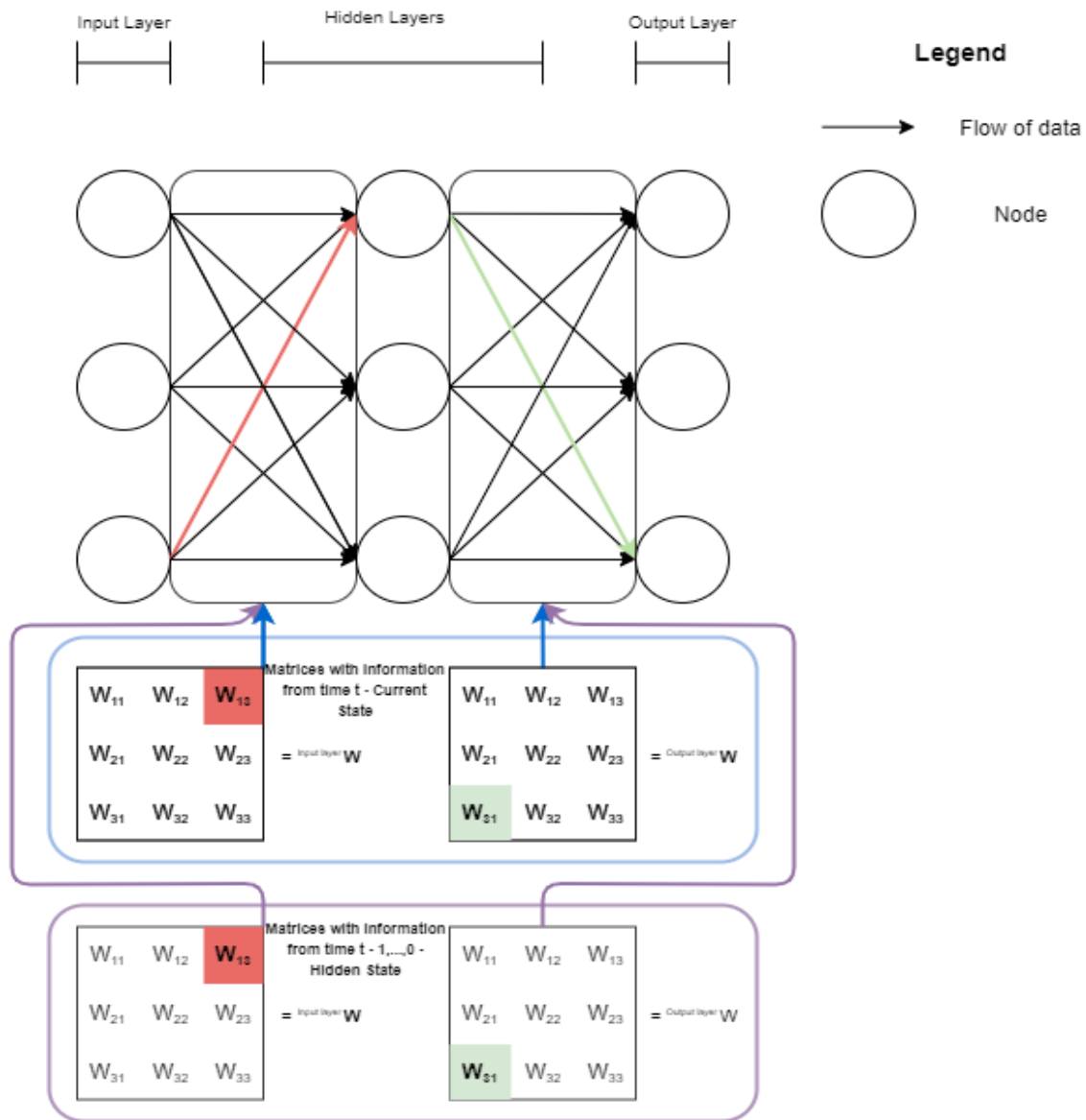
$$\mathbf{H}_t = \alpha \left(\left((\mathbf{X}_t \mathbf{W}^0) \cdots \right) \mathbf{W}^p + \left((\mathbf{H}_{t-1} \mathbf{W}_h^0) \cdots \right) \mathbf{W}_h^p \right) \quad (16)$$

269 where $\mathbf{X}_t \in \mathbb{R}^d$, $\mathbf{H}_{t-1} \in \mathbb{R}^d$, and the following $d \times d$ matrices: $\mathbf{W} = \{W_{ij}\}$ and $\mathbf{W}_h =$
 270 $\{W_{h:ij}\}$ for $i, j \in \{1, 2, \dots, d\}$.



271

272 Figure 7: Weights of a feedforward network, without recurrent connections

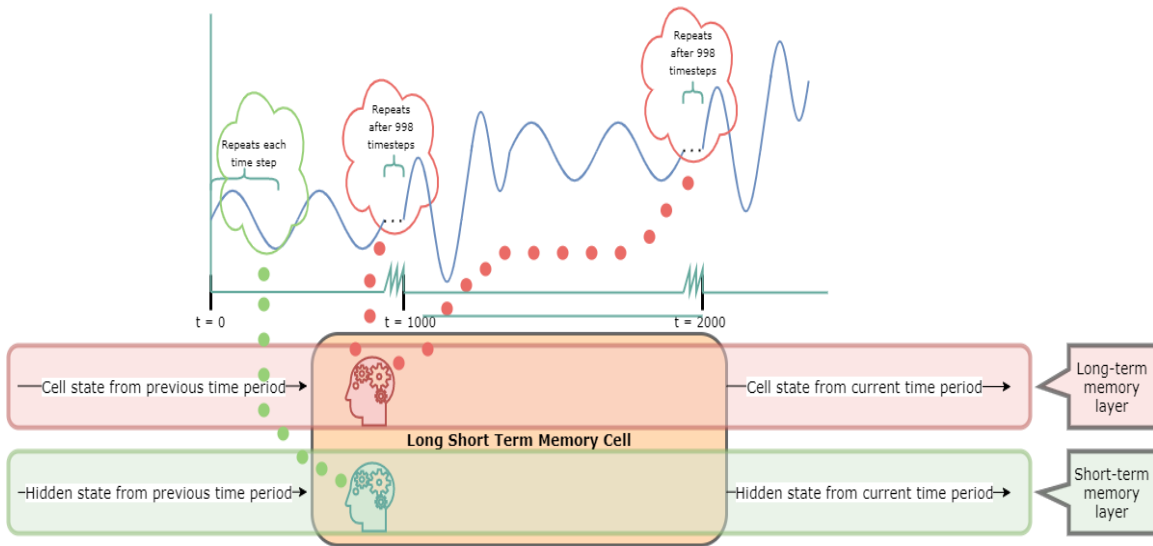


274

275 Figure 8: Weights of a feedforward network, with recurrent connections

276 4 Long Short Term Memory Cell (LSTM)

277 A recent innovation in RNN has been Long Short Term Memory (LSTM). The fun-
 278 damental reason for LSTM preference in sequence prediction is the ability of LSTM
 279 cells to learn relevant information in long input sequences (Sherstinsky, 2020, 1).



280

281

282

Figure 9: How LSTM handles short and long term dependencies

283

284

285

286

287

288

289

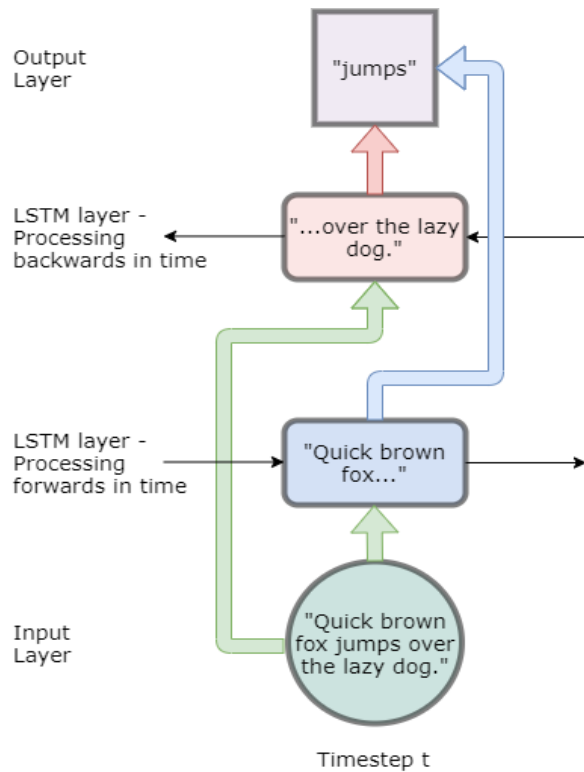
290

291

292

293

As a LSTM cell is fed with a sequence of data, it continuously changes its state and in doing so, it changes its long-term and short-term memory. Figure 9 shows more of the anatomy of a LSTM cell. The main idea behind an LSTM cell is its ability to overcome the 'short term' memory issues of the plain RNN architecture. How it accomplishes this is by having two dedicated parts in its memory, one for short and one long term pattern identification. 'Cell state' refers to the long term memory and the 'Hidden state' refers to the short term memory. As seen in Figure 9, there is a sinusoidal wave, which has a sudden amplitude change at every 1000 time steps. With plain RNNs, the sine wave that repeats every time step will be learned well but the sudden change at the longer time interval will be missed. LSTMs however do not suffer from this fate.



The sentence : "Quick brown fox jumps over the lazy dog."

294

295

Figure 10: How bidirectional LSTMs get data

296 As shown in Figure 10, bidirectional LSTMs consume data in both directions. This
 297 helps to establish context better because not only previous timestamps are used,
 298 but also data from future time stamps can also be used to predict outcomes. As
 299 shown with the dummy sentence, "Quick brown fox jumps over the lazy dog," the
 300 prediction uses data fed in both directions: backwards and forwards (Basaldella
 301 et al., 2018, 182-183). It is important to note that bidirectional data feeding only
 302 happens during training. During inference, we do not know what the future se-
 303 quences are for certain.

304 5 Main Research Idea

305 5.1 The Crux of the problem

306 Let us consider a set of independent companies labeled $\{0, 1, \dots, b\}$. Each com-
 307 pany provides cumulative loss development (CLD) data, with consecutive accident
 308 years (AYs) labeled $\{0, 1, \dots, m\}$ and development years (DYs) labeled $\{0, 1, \dots, n\}$ and

309 $m \geq n$ where m is the current year. Let C_{kij} denote the cumulative paid losses for
 310 k^{th} company, originating in the i^{th} accident year and at the j^{th} development year,
 311 where $i \in \{0, 1, \dots, m\}$, $j \in \{0, 1, \dots, n\}$, and $k \in \{0, 1, \dots, b\}$.

Table 3: Cumulative paid losses of company k

Accident Year (AY)	Development Year (DY)				
	0	...	g	...	n
312 0	$C_{k,0,0}$...	$C_{k,0,g}$...	$C_{k,0,n}$
1	$C_{k,1,0}$...	$C_{k,1,g}$...	$C_{k,1,n}$
...
h	$C_{k,h,0}$...	$C_{k,h,g}$...	$C_{k,h,n}$
...
m	$C_{k,m,0}$...	$C_{k,m,g}$...	$C_{k,m,n}$

313 Consider Table 3 which shows the cumulative paid losses of a P&C company.
 314 For the purposes of generalizing this table over a number of the companies of the
 315 same line of business, let's consider the k^{th} company. Claims for each accident year
 316 develops over n development years (also called lags). After the n^{th} lag period from
 317 the accident year, we assume that claims from that respective accident year are
 318 considered closed, i.e: the claims have matured and reached the ultimate losses
 319 so that no more claims can arise from accidents that took place in this specific ac-
 320 cident year (Radtke, 2016). We consider the most recent accident year which we
 321 have data as the m^{th} accident year. This implies that for the m^{th} accident year, we
 322 only have claims information for a single lag period, i.e. losses have only had one
 323 time period to develop. Therefore for any accident year, h ($h < m$), it is easy to
 324 see that we have $n - h$ unobserved loss developments periods. This means that for
 325 the h^{th} accident year, the last observable cumulative paid loss is $C_{k,h,n-h}$ (Schmidt,
 326 2016). If $m = n$, this gives us a cumulative paid loss development run-off triangle,
 327 for the k^{th} company, as shown in Table 4 below. Note that Table 4 shows a loss tri-
 328 angle that an insurance company typically faces. As can be seen, certain accident
 329 years have unobserved cumulative paid losses and the first unobserved cumulative
 330 paid loss occurs at $C_{k,h,n-h+1}$.

Table 4: A sample loss triangle - cumulative paid losses of company k

Accident Year (AY)	Development Year (DY)					
	0	1	...	g	...	n
0	$C_{k,0,0}$	$C_{k,0,1}$...	$C_{k,0,g}$...	$C_{k,0,n}$
1	$C_{k,1,0}$	$C_{k,1,1}$...	$C_{k,1,g}$...	
...		
h	$C_{k,h,0}$	$C_{k,h,1}$...	$C_{k,h,g}$		
...			
m	$C_{k,m,0}$					

331

332 Note that for $h = 0$, there are no unobserved cumulative paid losses as this is the
 333 oldest accident year on record and that since we expect the oldest accident year to
 334 be fully matured in terms of loss development, we already know the ultimate loss
 335 for the accident year $h = 0$. Conversely, $g = 0$ (i.e. the first lag period for any given
 336 accident year) would always be observable as each lag period data is assumed to be
 337 as of the end of that lag period. By estimating these unobserved cumulative paid
 338 losses, our final objective is to estimate the final cumulative paid loss for company
 339 k , i.e.:

$$\text{Final Cumulative Paid Loss} = C_{k,h,n} \quad (17)$$

340 where $h \in \{0, 1, \dots, m\}$. Table 5 demonstrates cumulative paid losses, including the
 341 ultimate paid losses that need to be estimated. Therefore, for the h^{th} accident
 342 year, the cumulative paid losses which need to be estimated before estimating the
 343 ultimate paid loss can be represented as shown in Table 5, where $t \in \{n-h+1, \dots, n-$
 344 $1\}$.

Table 5: The incomplete portion of the loss triangle in Table 4
Cumulative paid losses of company k

Accident Year (AY)	Development Year (DY)					
	0	1	\dots	g	\dots	n
0						\dots
1						$C_{k,1,n}$
\dots					\dots	\dots
h					\dots	$C_{k,h,n}$
\dots			\dots	\dots	\dots	\dots
m		$C_{k,m,1}$	\dots	$C_{k,m,g}$	\dots	$C_{k,m,n}$

5.2 Interdependencies in the Data

Besides the primary assumption of loss development being limited to n loss development periods, the secondary assumption that we make with regards to our data is that all run-off triangles are sourced from a common loss development environment. In other words, each run-off triangle is from a company that belongs to one particular line of business. For instance, medical malpractice, commercial auto, or workers' compensation. This secondary assumption enables us to combine and analyze loss development patterns in a more cohesive manner, leveraging certain techniques of machine learning to increase our sample size, rather than just looking at a single run-off table for a given company when making estimates. We can simultaneously look at run-off tables of several companies and jointly predict the loss development of these companies. We can further analyze this idea as follows. For a given company k , we have the following loss development run-off triangle already given in Table 4. For a given accident year h , $C_{k,h,g-1} \leq C_{k,h,g}$ for $g \in \{1, \dots, n\}$. This implies the existence of a latent function, $\xi(\cdot)$, such that

$$C_{k,h,g} = \xi(C_{k,h,g-1}) \quad (18)$$

Therefore, we can hypothesize that there is a latent function which takes a given cumulative paid loss of a given company at a certain accident year, to produce the cumulative paid loss of the next lag period, for the same company at the same accident year.

Due to our secondary assumption, we can assume that there exists some distri-

366 bution that can model the loss development of an h^{th} accident year, AY^h . The h^{th}
 367 accident year of any company therefore, can be assumed to be from the AY^h distri-
 368 bution. This assumption is plausible because we assume that since the companies
 369 that we are examining are from the same line of business, their loss experience is
 370 from a shared business/economic/regulatory environment. Thus, the loss devel-
 371 opment of each company, at a given accident year should be comparable to other
 372 companies.

373 If we take an order statistics approach, then AY^h distribution's g^{th} order statis-
 374 tic, which we denote as $AY_g^{(h)}$, can give us the $C_{k,h,g}$ for a given company k . We have
 375 to adjust AY^h such that idiosyncrasies of loss development of individual compa-
 376 nies are not ignored. Therefore, the distribution of interest is $AY^{(h|k)}$, i.e. loss
 377 development of the h^{th} accident year, for a given company k . The inverse run-off
 378 triangle for $AY^{(h|k)}$ is shown by Table 6:

Table 6: Inverse run-off triangle for $AY^{(h|k)}$

Accident Year (AY)	Development Year (DY)					
	0	1	...	g	...	n
0						
1						$AY_n^{(1 k)}$
...				
h					...	$AY_n^{(h k)}$
....		
m		$AY_1^{(m k)}$	$AY_g^{(m k)}$...	$AY_n^{(m k)}$

380 Thus in order to predict the ultimate losses for each company, we would need
 381 to know $AY_n^{(h)}$ for $h \in \{0, 1, \dots, m\}$ and n is the last lag period, for each company.
 382 However, we are no longer restricted to looking at only company specific data
 383 when modeling the loss development of a particular company. Let $R_{k,h,g}$ denote
 384 the ratio of the adjacent cumulative paid losses in columns g and $g - 1$, i.e.,

$$R_{k,h,g} = \frac{C_{k,h,g}}{C_{k,h,g-1}} \quad (19)$$

385 where $g = 1, 2, \dots, n - 1$ and h is the accident year. Transforming the data in this
 386 manner helps approximately normalize data in a manner which is frequently used

387 by actuaries. In addition, the ratios also tend to fluctuate within a smaller range
 388 than non-normalized loss numbers, as shown in Table 7.

Table 7: Inverse run-off triangle using loss development ratios

Accident Year (AY)	Development Lag (DY)							
	0	1	\dots	g	\dots	$n-j$	\dots	$n-1$
0								
1								$R_{k,1,n-1}$
\dots						\dots	\dots	\dots
h						$R_{k,h,n-j}$	\dots	$R_{k,h,n-1}$
				\dots	\dots	\dots	\dots	\dots
m		$R_{k,m,1}$	\dots	$R_{k,m,g}$	\dots	$R_{k,m,n-j}$	\dots	$R_{k,m,n-1}$

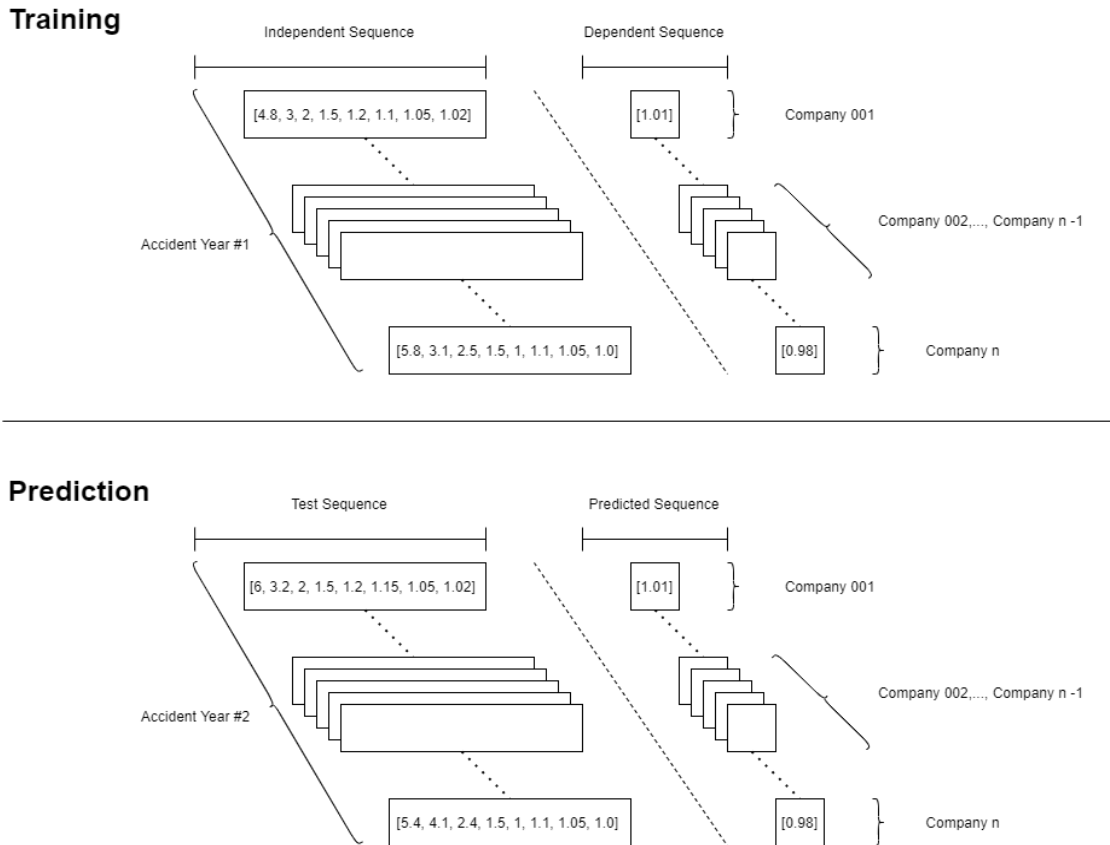
390 6 Modeling the data

391 The composite model built in this paper needs the input data to adhere to some
 392 important assumptions:

- 393 1. As per the case with this data set, we assume that no more losses are incurred
 394 after 10 years (Meyers & Shi).
- 395 2. The loss development pattern of each accident year should be relatively com-
 396 parable, i.e. the loss development pattern of each accident year should con-
 397 tain similar levels of noise. If each accident year's loss development has in-
 398 comparable noise levels, predictions lose reliability (Giles et al., 2001).

399 The model of choice for this paper is a composite model which is made of 8
 400 sub-models, making 8 sequence predictions in total. The predictions are recursive
 401 in nature with each prediction building on the preceding predictions. Because the
 402 loss triangle is an inverted right angle triangle, in order to build a complete square
 403 out of the triangle, we need to progressively increase the length of the prediction
 404 sequence. We start with the predictions for the first accident year, i.e. the topmost
 405 row of the loss triangle. There is nothing to predict in this row. However, we
 406 can feed all lag periods barring the last, as a single sequence. This can act as
 407 our independent variable. The last lag period can be input into the model as the
 408 dependent variable. For both independent and dependent sequences, each stripe

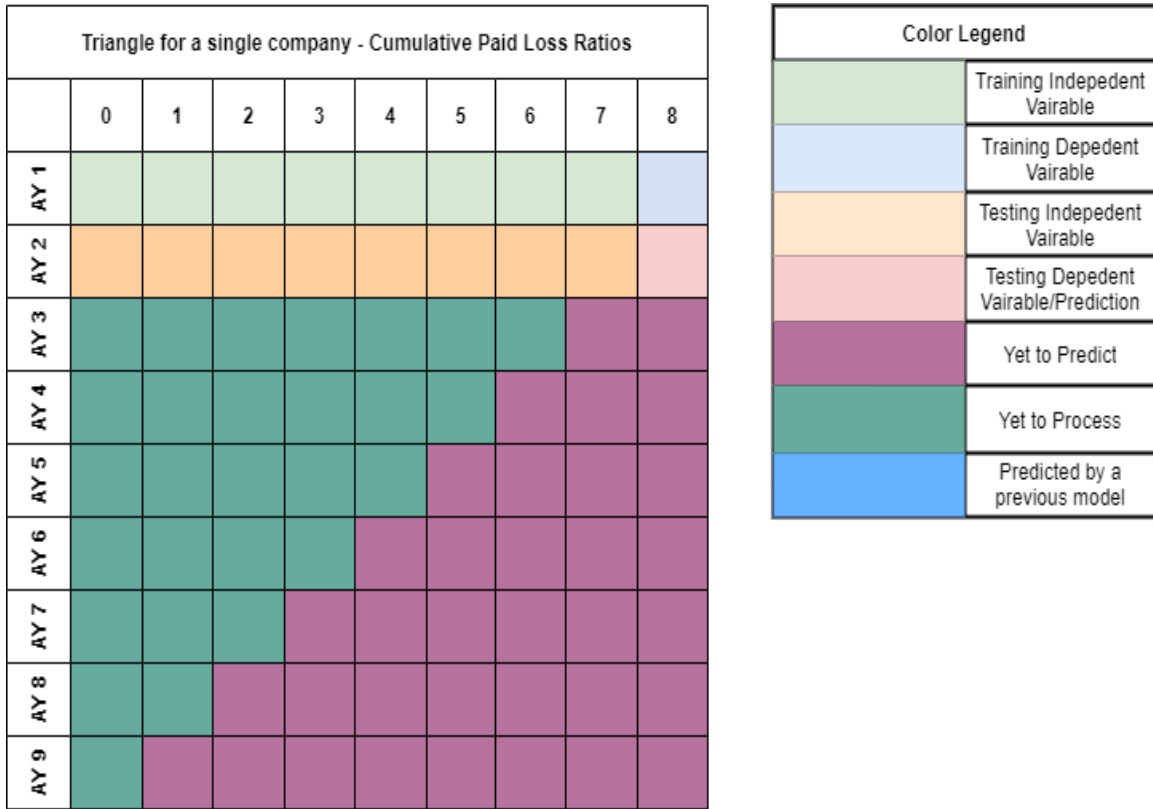
409 of a sequence represents data relates to a single company. For instance, the loss
 410 sequence of Company 001 is represented together by the topmost rectangle on the
 411 left and the topmost square on the right, in the ‘Training’ portion of Figure 11.
 412 It must be noted that this model building process does not aim to complete the
 413 loss triangles by completing the diagonals. Instead we build out each row, from
 414 the rows with the most complete sequences (mature data), to those with the least
 415 complete sequences (newer data).



416
 417 Figure 11: Feeding data into a sub-model 1

418 We can then use the second accident year’s loss sequence, from the first to the
 419 penultimate lag as the ‘test’ independent variable. The ‘Prediction’ portion of Fig-
 420 ure 11 shows this. Since we want to predict the last lag period’s loss development
 421 of the second accident year (this will be our first ‘true’ prediction), we will train
 422 our model with the loss sequence from the previous accident year and use that to
 423 predict the succeeding accident year’s loss development. For any given company,
 424 using the structure shown in Figure 11, we can arrive at a partially completed loss
 425 rectangle as shown in Figure 12.

426

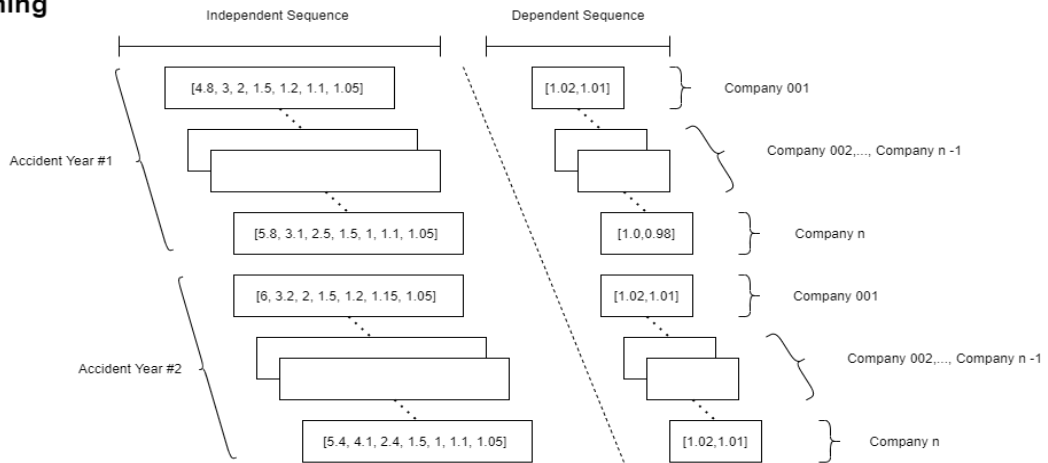


427

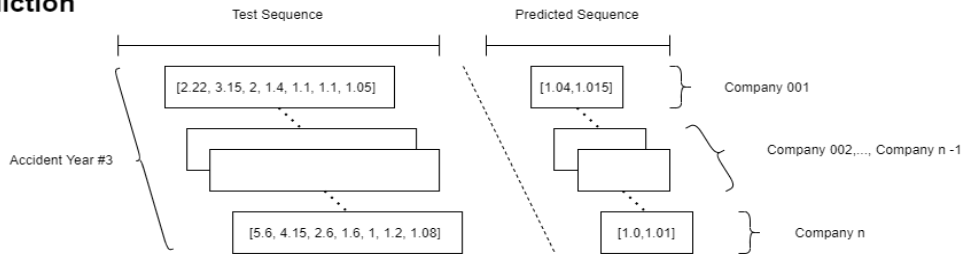
428 Figure 12: Partially completed loss square, after the predictions made using
 429 sub-model 1

430 After the first sub-model has been made, we use all our previously completed
 431 sequence data to make the new dependent and independent loss sequences. We
 432 look to see the length of the sequence that we have to predict and then we treat
 433 our previous accident years' data as input. Each accident year is treated as a sam-
 434 ple. Figure 13 demonstrates this. In the second sub-model, we have to predict a
 435 dependent sequence that is 2 periods in length and we use the first two accident
 436 years of data. For any given company, using the structure shown in Figure 13, we
 437 can arrive at a partially completed loss square as shown in Figure 14. Note that
 438 the prediction shown in Figure 13 uses predictions made by process shown in the
 439 Figure 11.

Training



Prediction

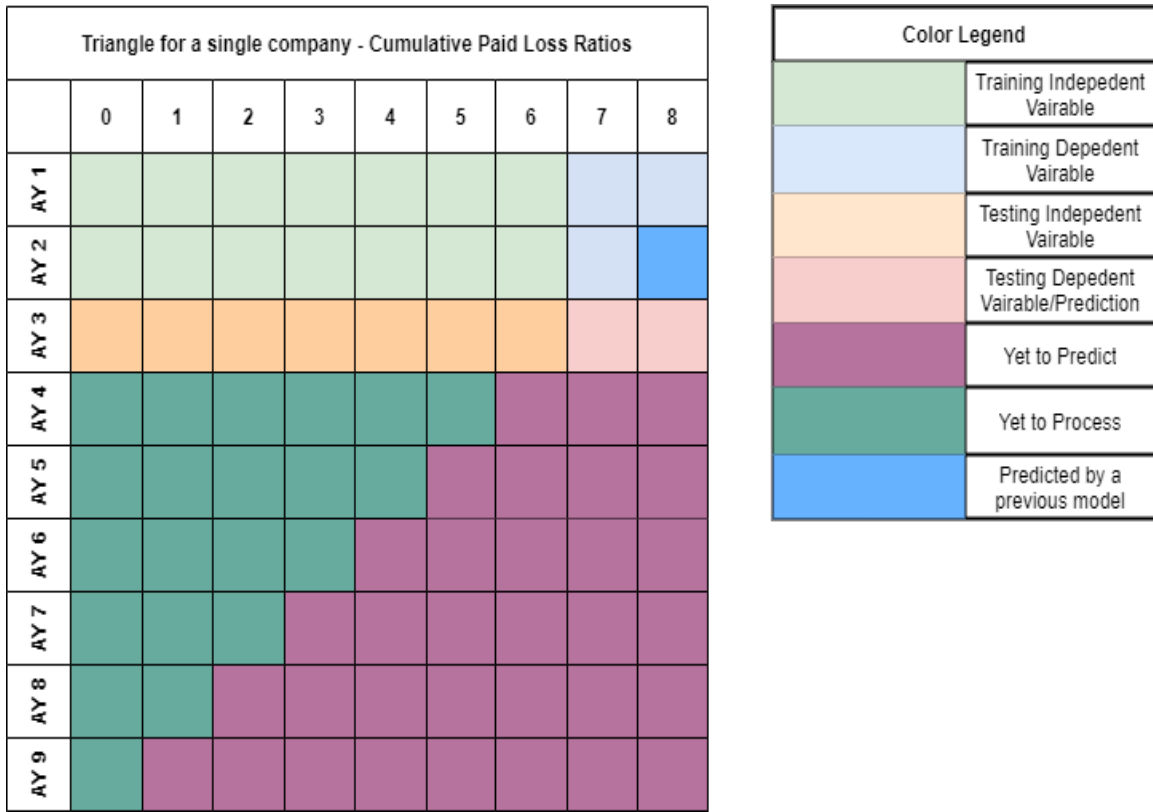


440

441

Figure 13: Feeding data into a sub-model 2

442

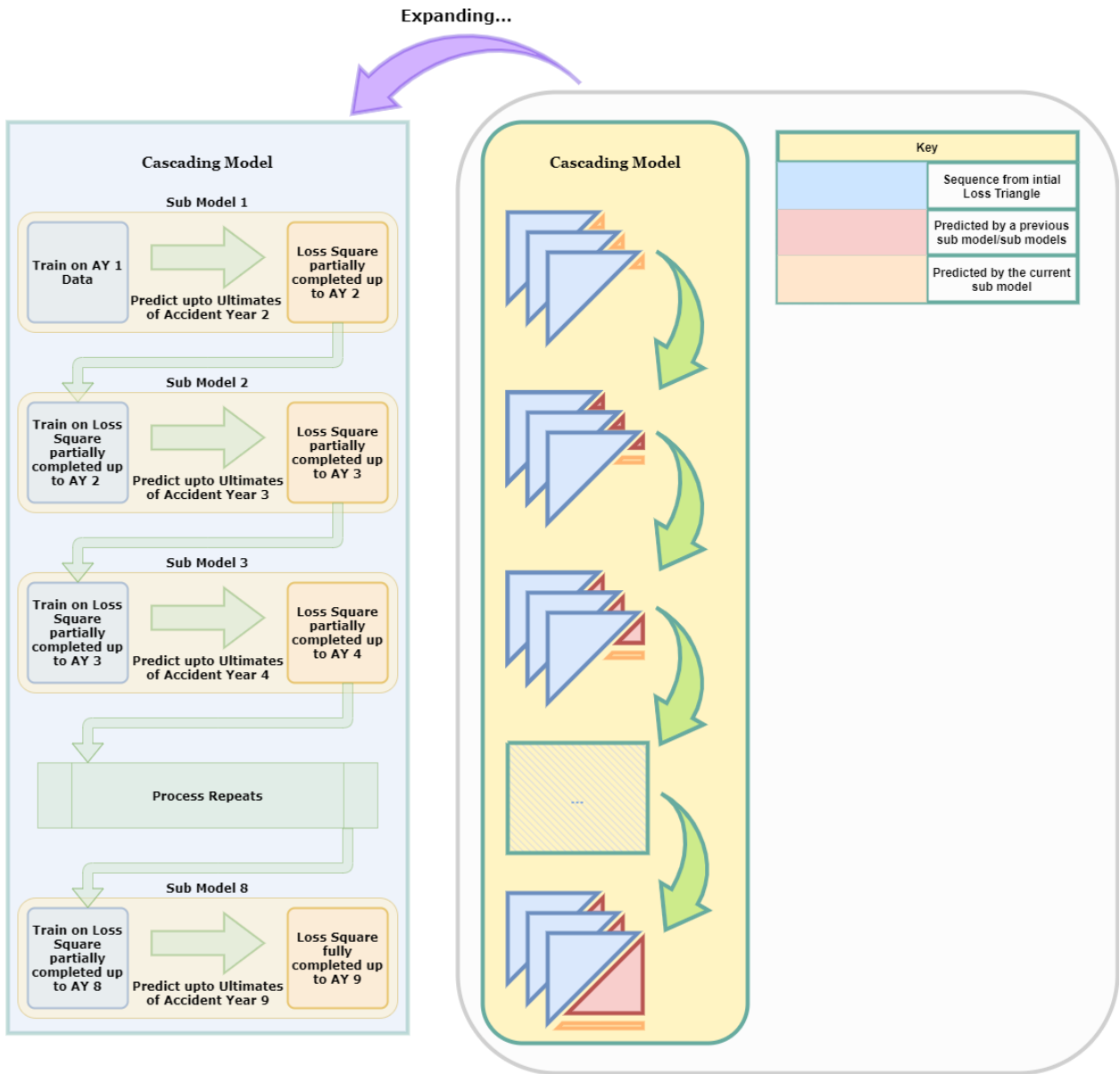


443

444 Figure 14: Partially completed loss square, after the predictions made using
 445 sub-model 2

446 We can generalize the process of building sub-models based on other sub-
 447 models, as highlighted in the building of the first sub-model followed by the sec-
 448 ond sub-model. This can be referred to as ‘Cascading’ (Harej et al., 2017). This is
 449 illustrated in Figure 15. With reference to Figure 15, the bigger stacked triangles
 450 represent the loss triangles of each company in the data set. The first sub-model
 451 predicts the ultimate losses of the second accident year of the data set.

452



453

454

Figure 15: General process of cascading

455 6.1 The Training Data

456 To successfully implement our deep learning approach, we need so-called train-
 457 ing data. This is further explained in Section 2. The training data can be split
 458 into two parts: The first part is the independent training sequence while the sec-
 459 ond part deals with the dependent training variable. To implement the first part,

460 let S_r^{ITRM} denote independent training matrix (ITRM), S_r^{DTRM} denote dependent
461 training matrix (DTRM), S_r^{ITSM} independent test matrix (ITRM), S_r^{POM} denote pre-
462 dicted output matrix (POM), for sub-model r , for $r = 1, 2, \dots, 8$. For $R_{k,h,g}$ defined
463 in equation (19) with $k = 0, 1, \dots, b$, $h = 0, 1, \dots, m$, and $g = 0, 1, \dots, n$, S_1^{ITRM} looks at
464 the most mature (or oldest) losses and is given by:

$$S_1^{\text{ITRM}} = \begin{bmatrix} R_{0,0,0} & \cdots & R_{0,0,n-1} \\ \vdots & \vdots & \vdots \\ R_{b,0,0} & \cdots & R_{b,0,n-1} \end{bmatrix} \quad (20)$$

465 The second part of the training data is the dependent training matrix (DTRM),
466 S_1^{DTRM} , given by

$$S_1^{\text{DTRM}} = \begin{bmatrix} R_{0,0,n} \\ \vdots \\ R_{b,0,n} \end{bmatrix} \quad (21)$$

467 The matrix described in 20 represents the oldest losses (losses at accident year
468 0), from the lag periods 0 through $n - 1$ ($n - 1 = 8$ in this case), for each company
469 present in the dataset. The matrix shown in 21 contains the final loss ratio. To-
470 gether these 2 matrices - S_1^{ITRM} and S_1^{DTRM} , form an independent and dependent
471 relationship. This relationship is what is detected by the deep learning algorithm.
472 Once the first sub-model is trained with the above data, we can get the first pre-
473 diction. We predict with test data. Test data can also be broken into two parts as
474 before; independent and dependent. The independent test data can be shown as:

$$S_1^{\text{ITSM}} = \begin{bmatrix} R_{0,1,0} & \cdots & R_{0,1,n-1} \\ \vdots & \vdots & \vdots \\ R_{b,1,0} & \cdots & R_{b,1,n-1} \end{bmatrix} \quad (22)$$

475 The dependent test data or the predicted ultimate loss ratios, are given by the
476 predicted output matrix (POM), S_1^{POM} where

$$S_1^{\text{POM}} = \begin{bmatrix} R_{0,1,n} \\ \vdots \\ R_{b,1,n} \end{bmatrix} \quad (23)$$

477 With the test data, in a similar fashion to the training data, we can divide the
478 data into independent and dependent data. In this case, we seek to predict the final

479 loss ratio, for each company in the dataset. Since the Deep Learning algorithm has
 480 already been fed with training data, both dependent and independent data - we
 481 only need to provide the algorithm independent testing data. With the patterns
 482 extracted from the training data using the oldest losses, the sub-model 1 is able to
 483 predict the ultimate loss ratio using the loss sequence of the second oldest accident
 484 year. Note that the independent data for both training and test data are of the same
 485 length, over identical lag periods. The only difference is that with test data, we do
 486 not know the dependent value (this is also the first lag which we do not know of,
 487 as the second oldest accident year takes one more lag period to fully mature), and
 488 therefore this is the matrix we will predict.

489 The second sub-model therefore processes the two oldest accident years - the
 490 two topmost rows of the loss triangle. The second row contains predictions from
 491 the previous sub-model. The two rows are split into training data, testing data,
 492 and predicted data. The second sub-model can be written as:

$$S_2^{\text{ITRM}} = \begin{bmatrix} [R_{0,0,0} \cdots R_{0,0,n-2}] \\ \vdots \\ [R_{b,0,0} \cdots R_{b,0,n-2}] \\ [R_{0,1,0} \cdots R_{0,1,n-2}] \\ \vdots \\ [R_{b,1,0} \cdots R_{b,1,n-2}] \end{bmatrix} \quad (24)$$

493 S_2^{ITRM} is the independent training data matrix. The second part of the training
 494 data is the dependent training matrix, S_2^{DTRM} , given by

$$S_2^{\text{DTRM}} = \begin{bmatrix} [R_{0,0,n-1} \quad R_{0,0,n}] \\ \vdots \\ [R_{b,0,n-1} \quad R_{b,0,n}] \\ [R_{0,1,n-1} \quad R_{0,1,n}] \\ \vdots \\ [R_{b,1,n-1} \quad R_{b,1,n}] \end{bmatrix} \quad (25)$$

495 Once the second sub-model is trained with the above data, we can get the sec-
 496 ond prediction. Note that in the second sub-model, our goal is to predict the last
 497 two lag ratios of the third accident year or third row, for each company. Therefore,
 498 our dependent matrix of our training data is two lag periods wide, since we need

499 to train to predict the last two lag periods. This means that the matrix of our inde-
 500 pendent training data can only be $n - 2$ ($n - 2 = 7$ in our case) elements wide. Test
 501 data can also be broken into two parts as before; independent and dependent. The
 502 independent test data can be shown as:

$$S_2^{\text{ITSM}} = \begin{bmatrix} R_{0,2,0} & \cdots & R_{0,2,n-2} \\ \vdots & \vdots & \vdots \\ R_{b,2,0} & \cdots & R_{b,2,n-2} \end{bmatrix} \quad (26)$$

503 Note that the S_2^{ITRM} is identical to S_2^{ITSM} in width, whilst S_2^{DTRM} is identical to
 504 S_2^{POM} in width. This is done for the same reasons as in the sub-model 1 training
 505 - the algorithm knows the nature and dimensions of the independent and depen-
 506 dent relationships of the data for the third accident year. The dependent test data
 507 or the predicted ultimate loss ratios can be shown as:

$$S_2^{\text{POM}} = \begin{bmatrix} R_{0,2,n-1} & R_{0,2,n} \\ \vdots & \vdots \\ R_{b,2,n-1} & R_{b,2,n} \end{bmatrix} \quad (27)$$

508 Following this pattern, the last sub-model, which predicts the ultimates of the
 509 last accident year is given as follows:

$$S_8^{\text{ITRM}} = \begin{bmatrix} \begin{bmatrix} R_{0,0,0} \\ \vdots \\ R_{b,0,0} \end{bmatrix} \\ \vdots \\ \begin{bmatrix} R_{0,m-1,0} \\ \vdots \\ R_{b,m-1,0} \end{bmatrix} \end{bmatrix}, \quad (28)$$

510 the independent training variable is:

$$S_8^{\text{DTRM}} = \begin{bmatrix} \begin{bmatrix} R_{0,0,1} & \cdots & R_{0,0,n} \\ \vdots & \vdots & \vdots \\ R_{b,0,1} & \cdots & R_{b,0,n} \end{bmatrix} \\ \vdots \\ \begin{bmatrix} R_{0,m-1,1} & \cdots & R_{0,m-1,n} \\ \vdots & \vdots & \vdots \\ R_{b,m-1,1} & \cdots & R_{b,m-1,n} \end{bmatrix} \end{bmatrix}, \quad (29)$$

511 the dependent testing data matrix is:

$$S_8^{\text{DTRM}} = \begin{bmatrix} R_{0,m,0} \\ \vdots \\ R_{b,m,0} \end{bmatrix} \quad (30)$$

512 and the predicted output matrix is:

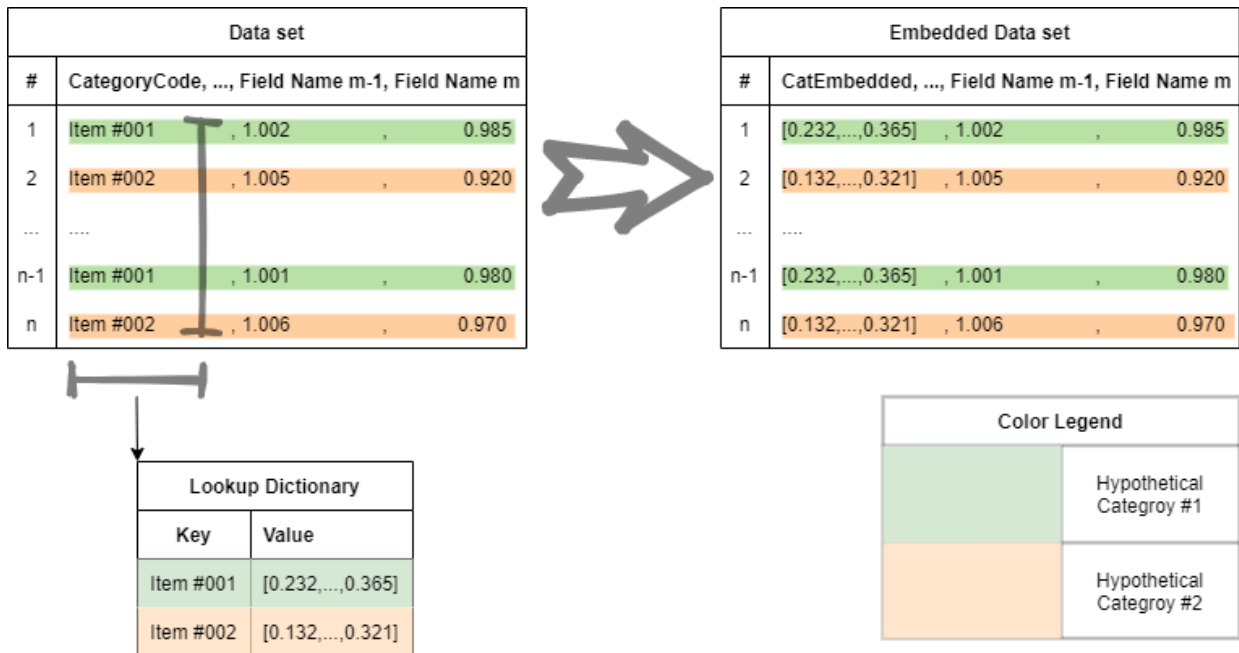
$$S_8^{\text{POM}} = \begin{bmatrix} R_{0,m,1} & \cdots & R_{0,m,n} \\ \vdots & \vdots & \vdots \\ R_{b,m,1} & \cdots & R_{b,m,n} \end{bmatrix}. \quad (31)$$

513 Once all sub-models have made their predictions, the loss development trian-
514 gle for each company can be completed and the loss reserves can be estimated.

515 6.2 Role of Embedding

516 The process highlighted in Section 6.1 is a demonstration of how cascading works
517 with sub-models in order to create a comprehensive overall model. However, cas-
518 cascading by itself does not help to create an overall modeling process that can predict
519 the loss development of multiple companies at once. As highlighted in Section 6.1,
520 when we input data into the sub-models, we do recognize that the data comes from
521 multiple companies. However, this alone is not enough to ensure that the neural
522 network is aware that it is dealing with parallel sequences of losses from different
523 companies. For that, we need to ensure that we use embedding on each paral-
524 lel sequence that we input. Embedding is a means to replace original categorical
525 identification data such as categorical names, with vectors (Google, 2021). These
526 vectors are deep learning friendly. This process is shown in Figure 16.

527



528

529

Figure 16: Process of Embedding

530 Embedding is done by first creating a lookup dictionary as shown. Initially, each
 531 category is regarded as a key and a subsequent random vector is made for that
 532 key in the dictionary. This random vector then replaces each original entry of
 533 the categorical name in the data set. By replacing each categorical name with a
 534 vector, the substituting vector can be treated like any other variable of the deep
 535 learning model. This enables the deep learning algorithm to create a matrix of
 536 vectors of length j , where j is the total number of categories in the data, and a
 537 width of w , where w is the length of each row, i.e., length of vector representing
 538 each embedded category.

539 7 Sub-Model Architectures

540 Each sub-model has identical architectures, with the difference being in the size
 541 of the input sequences, length of company codes list, the number of bidirectional
 542 layers, dense layers, and the width of the output layer. In building a cascading
 543 model, the biggest challenge was to build sub-models that progressively increased
 544 in the number of parameters in such a way that the respective sub-models did
 545 not overfit the data. Hence the reason why the number of bidirectional layers and

546 dense layers gradually increase with the amount of input data. Table 8 gives a
 547 brief technical description of the deep learning components used in making each
 548 sub-model.

Table 8: Summary of the major architectural decisions of each sub-model

Submodel Component	Description
Bidirectional LSTM Layer	Activation used = Softplus, Recurrent Dropout used.
Dense Layer (Non-output)	Activation used = SELU, Activity Regularizer l1 and l2 used.
Dense Layer (Output)	No activation or Activity Regularization used
Optimizer	Nadam with MAPE as the loss function
Call Backs	Early Stopping at 50 epochs

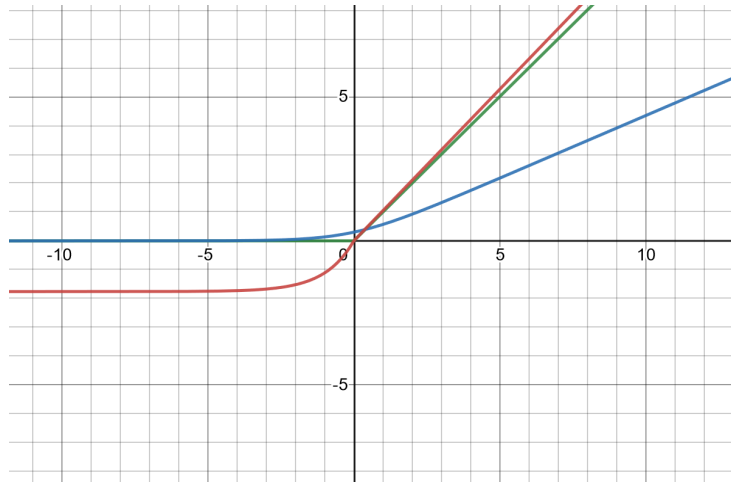
550 Softplus is not as widely used as some other activation functions such as the Rec-
 551 tified Exponential Linear Unit (RELU). However, on this data set, Softplus tends
 552 to perform better than some of the other activation functions, for optimizing us-
 553 ing LSTM cells. In terms of the anatomy, Softplus is very similar to RELU with the
 554 minor difference of being smoother close to the Input = 0 region. Figure 17 shows
 555 these functions. The Scaled Exponential Linear Unit (SELU) activation function is
 556 used in the dense layers, with the exception of the output layer. The SELU activa-
 557 tion function, much like the Softplus activation, was used due to its performance
 558 on the data set. The formulas for each activation function is as follows (Nwankpa
 559 et al., 2018):

$$\text{RELU: } f(x) = \begin{cases} 0 & \text{if } x < 0 \\ x & \text{if } x \geq 0, \end{cases} \quad (32)$$

$$\text{Softplus: } f(x) = \log_{10}(e^x + 1) \quad x \in \mathbb{R} \quad (33)$$

560 and

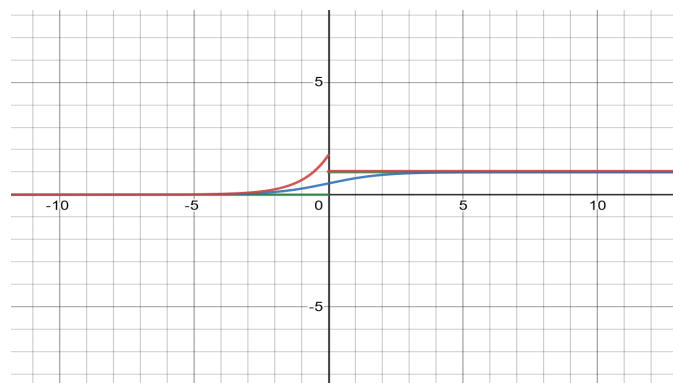
$$\text{SELU: } f(x) = \begin{cases} 1.05070098x & \text{if } x < 0 \\ 1.05070098 \times 1.67326324(e^x - 1) & \text{if } x \geq 0 \end{cases} \quad (34)$$



561

562 Figure 17: Activation functions used: Softplus (Blue), SELU (Red), RELU (Green)

563 Since sequence processing involves repeatedly taking derivatives of activation
 564 functions, saturation regions in activation functions can lead to vanishing or ex-
 565 ploding gradients (Pascanu et al., 2012). The derivatives of Figure 18 show that
 566 for values of input (horizontal axis) close to 0 - for any neuron cell, saturation does
 567 not occur in Softplus. Perhaps the smooth gradient around 0 in the derivative of
 568 Softplus may assist in detecting patterns specific to this data set, hence explain-
 569 ing its better performance. However, further research is needed to confirm this.
 570 One similarity between the derivatives of Softplus and SELU is that they do not
 571 immediately saturate in the periphery of 0. This could be a potential reason for
 572 their good performance on this data set.



573

574 Figure 18: Derivatives of activation functions used: Softplus (Blue), SELU (Red),
 575 RELU (Green)

576 The loss function of choice for sequence prediction is mean absolute percentage

577 error (MAPE). This loss function is preferred as the percentage deviation is an eq-
578 uitable measure of deviation, regardless of the normalization used in the sequence
579 (de Myttenaere et al., 2015). In our case, as the data used is ratio data, using the
580 more commonly used mean squared error (MSE) loss function will produce very
581 small errors which may be trickier to optimize. The MAPE loss function is given
582 by:

$$\text{MAPE loss function} = \arg \min_{\hat{\mathbf{y}}} \left(\frac{100}{n} \sum_{i=0}^n \left(\frac{\hat{y}_i - y_i}{y_i} \right) \right) \quad (35)$$

583 where $\mathbf{y} = (y_0, y_1, \dots, y_n)$ is the vector of observed or actual values and $\hat{\mathbf{y}} = (\hat{y}_0, \hat{y}_1, \dots, \hat{y}_n)$
584 is the vector of predicted or estimated values.

585 **8 Observations - Loss Development Factors and Acci-** 586 **dent Year/Development Year Interactions**

587 As already established, this model uses loss development factors and consumes
588 data by accident year - to complete each row of the loss triangles of the respective
589 companies. Even so, the business of extracting loss patterns is an endeavor fraught
590 with many dangers. In this section, we aim to consider some of these dangers
591 and also seek to establish the scope of the remedies that we have applied in our
592 approach to minimize these dangers. Loss development patterns can change due
593 to a myriad of reason (Clark et al., 2021):

- 594 • Change in the business mix of an insurance company, particularly but not
595 limited to the frequency and severity of claims.
- 596 • Changes in the procedures followed - for instance the process of establishing
597 a case reserve.
- 598 • Commutations where the re-insurer transfers its current and future liability
599 from particular ceded contracts back to the original insurer, along with an
600 agreed upon payment. This is a known phenomena impacting losses from
601 the Schedule P loss triangle - our data source.
- 602 • Missing or incomplete data.
- 603 • Changes in law and tort reform

- 604 • Social inflation causing increases in pay outs.

605 Data along diagonals, particularly from the later accident years when losses
606 have yet to mature, can become significantly distorted by the above highlighted
607 phenomena. Our model does not aim to tackle any of the above phenomena. Our
608 focus is to merely demonstrate a methodology that can detect and extract loss
609 development patterns. Whilst it is essential that the sources of loss pattern distor-
610 tions be identified, we feel that doing so in this paper would be a distraction to the
611 fundamental aim of the paper.

612 De-trending is another important aspect of pre-processing loss development
613 sequences. Whilst knowing the sources of loss distortions can be of immense help,
614 we do not necessarily require this knowledge to de-trend a loss sequence. In our
615 modeling approach, since we consider the loss patterns of all respective compa-
616 nies when making a prediction on any one company's loss pattern, we partially
617 immunize the model from being too overly sensitive to any idiosyncratic loss trend
618 present in only one company. By considering loss development on a row by row
619 basis, we also seek to partially immunize the model from fluctuations present at
620 the diagonal of each loss triangle. Hence our approach to de-trending is embed-
621 ded in our choice of setting up the model, and also on the inherent virtues of deep
622 learning via recurrent neural networks.

623 **9 The Main Results**

624 Table 9 shows the average deviation of the ultimate loss predictions for each ac-
625 cident year, across all companies, under each method. Deep Learning (DL) is the
626 method implemented in this paper. Chain Ladder is a Python package implemen-
627 tation of loss reserving that is already available for use (Chain Ladder - Reserving
628 in Python, 2021). The Chain Ladder Python package has a vast array of function-
629 alities beyond calculating ultimate losses, but for the purposes of this paper, we
630 use it to only calculate ultimate losses.

631 Table 9: Average deviation of predictions in percentages

632 Notes: CL refers to Chain Ladder and DL refers to Deep Learning

	AY 2	AY 3	AY 4	AY 5	AY 6	AY 7	AY 8	AY 9	AY 10
DL	0.00	1.03	3.60	7.46	6.51	9.00	13.77	25.40	30.86
CL	1.07	1.10	3.49	3.66	7.82	11.20	16.97	26.08	61.55

633 One important fact to highlight is that under the Chain Ladder package, there
634 is no need to calculate the loss development factors first. Therefore the loss tri-
635 angle can start developing from the first accident year. However, under the DL
636 method, since we are working with loss development factors, we have to consume
637 the first two accident years to develop the first ratio, the second two accident years
638 to develop the second ratio and soon. Therefore, in order to create loss data which
639 contain an equal number of lag periods and accident years, we need to omit the
640 first accident year. This is the reason for the AY2 having a prediction of deviation
641 of 0 under the DL method; there is no prediction to be made for AY2.

642 The prediction deviation is calculated as:

$$\text{Prediction deviation} = \frac{100}{n} \sum_{i=0}^n \left| \frac{\hat{y}_i - y_i}{y_i} \right| \quad (36)$$

643 An example of how the performance deviation is calculated under the Deep
644 Learning (DL) method can be illustrated as follows. Supposing we are interested
645 in the deviation of the 9th lag period of accident year 3 prediction (which is also
646 the Ultimate Loss of AY3).

Table 10: Sample cumulative paid loss development ratios, $\{s_0, \dots, s_8\}$

Actual loss square of a single company - Cum. Paid LDF									
	0	1	2	3	4	5	6	7	8
AY 3	3.665	2.220	1.530	1.040	1.020	1.010	1.000	0.980	1.000

647

Table 11: Sample predicted cumulative paid loss development ratios, $\{\hat{s}_0, \dots, \hat{s}_8\}$

Predicted loss square of a single company - Cum. Paid LDF									
	0	1	2	3	4	5	6	7	8
	...								
AY 3	3.665	2.220	1.530	1.040	1.020	1.010	1.000	0.980	1.030
	...								

648

649 The Tables 10 and 11 show a pair of sample tables, actual and predicted cu-
 650 mulative paid loss development ratio values respectively; for a sample company.
 651 These tables will be used to demonstrate how to calculate performance deviation
 652 under the Deep Learning method. The calculations are shown below. Suppose
 653 $\{s_1, \dots, s_i, \dots\}$ is a sequence of observed or actual values and $\{\hat{s}_1, \dots, \hat{s}_i, \dots\}$ is a se-
 654 quence of predicted or estimated values and j represents the lag period of evalua-
 655 tion. Then the performance deviation at the j^{th} lag is:

$$\text{Performance Deviation at Lag } j = \left| \frac{\prod_{i=0}^j \hat{s}_i - \prod_{i=0}^j s_i}{\prod_{i=0}^j s_i} \right| \quad (37)$$

656 so that the AY3 prediction deviation (at $j = 8$) becomes

$$\text{AY3 Prediction Deviation} = \left| \frac{\prod_{i=0}^8 \hat{s}_i - \prod_{i=0}^8 s_i}{\prod_{i=0}^8 s_i} \right| \quad (38)$$

657 Note that for AY3, Table 10 gives $\prod_{i=0}^8 s_i = 3.665 \times 2.220 \dots \times 1.00 = 13.0707$. On
 658 the other hand, for AY3, Table 11 gives $\prod_{i=0}^8 \hat{s}_i = 3.665 \times 2.220 \dots \times 1.03 = 13.4628$

659 The Tables 12 and 13 show a pair of sample tables, actual and predicted cu-
 660 mulative paid loss values respectively, for a sample company. These tables will
 661 be used to demonstrate how to calculate performance deviation under the Chain
 662 Ladder method. The calculations are shown below.

Table 12: Sample cumulative losses, $\{y_0, \dots, y_9\}$

Actual loss square of a single company - Cum. Paid Losses										
	0	1	2	3	4	5	6	7	8	9
	...									
AY 3	20.0	48.0	60.0	66.0	67.0	67.5	68.0	69.0	69.2	69.2
	...									

663

Table 13: Sample predicted cumulative paid losses, $\{\hat{y}_0, \dots, \hat{y}_9\}$

Predicted loss rectangle of a single company - Cum. Paid Losses										
	0	1	2	3	4	5	6	7	8	9
AY 3	20.0	48.0	60.0	66.0	67.0	67.5	68.0	69.0	69.2	69.5

664

$$\text{AY3 Prediction Deviation} = \left| \frac{\hat{y}_9 - y_9}{y_9} \right| = \left| \frac{69.5 - 69.2}{69.2} \right| = 0.433\%. \quad (39)$$

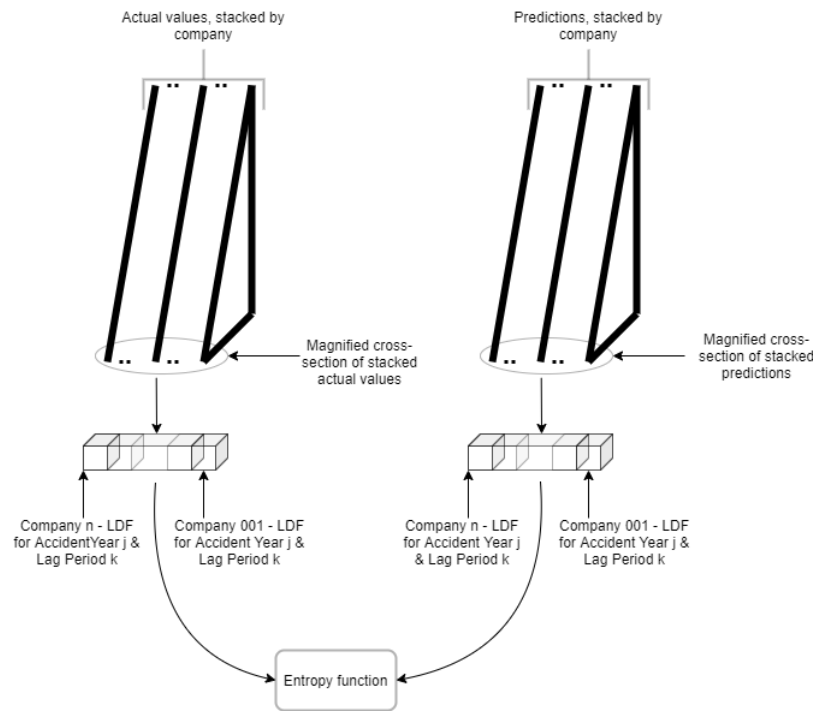
665 10 Closing Comments

666 10.1 Critique of the Inherent Model Limitations

667 Although the performance metrics shown in Table 9 show us the predictive perfor-
 668 mance of the overall model, these results do not give us a nuanced insight of the
 669 inherent weaknesses of the overall model. The nature of the assumptions which
 670 were made in section “Modeling the data”, along with how the loss data develops
 671 towards the tails, causes the burden of accuracy of the predictions to weigh heavily
 672 on the later sub-models as opposed to the earlier sub-models. This is because the
 673 later sub-models have to not only base their predictions on the ever propagating
 674 errors of the previous sub-models, but also predict longer sequences with shorter
 675 input sequences. This imposes a unique challenge in that the predictions need to
 676 account for ever increasing dynamism of data, as the longer into the future, short
 677 term trends may not be preserved well (Sánchez-Sánchez et al., 2019).

678 Unlike the beginnings of sequences, the loss development factors at the tails for
 679 almost all companies, regardless of the accident year, tend to approach and settle
 680 at 1.00. This is an instance of a “concept shift”, where the non-stationary nature
 681 of data causes the relationship of extracted features with predicted sequence to
 682 change over lag periods (Baier et al., 2020). This means that all sub-models can
 683 predict the tail well because the volatility of the tail is comparatively insignificant
 684 across all accident years and all companies, when compared to the volatility of loss
 685 development factors at the beginnings of the sequences. Under this scenario, the
 686 very nature of the ‘cascading’ structure of the overall model presents an inherent

687 limitation to how accurate the predictions of the later accident years can be. In
 688 order to study this in detail, the author turned to the entropy package from the
 689 `scipy` library. On the right, the predictions obtained from the overall model are
 690 stacked by company. At each lag period, and at each accident year, the loss devel-
 691 opment factors are extracted. The range of values obtained in this manner can be
 692 regarded as a distribution of sorts, unique to this particular lag period and acci-
 693 dent year. In a similar manner as explained before, the actual loss development
 694 factors at each lag period and each accident year, stacked by company, can be re-
 695 garded as a distribution. By comparing each pair of distributions, at each accident
 696 year - lag period pair, we develop a plot of the entropy at each respective point.
 697 The process of how this library is used is shown in Figure 19.



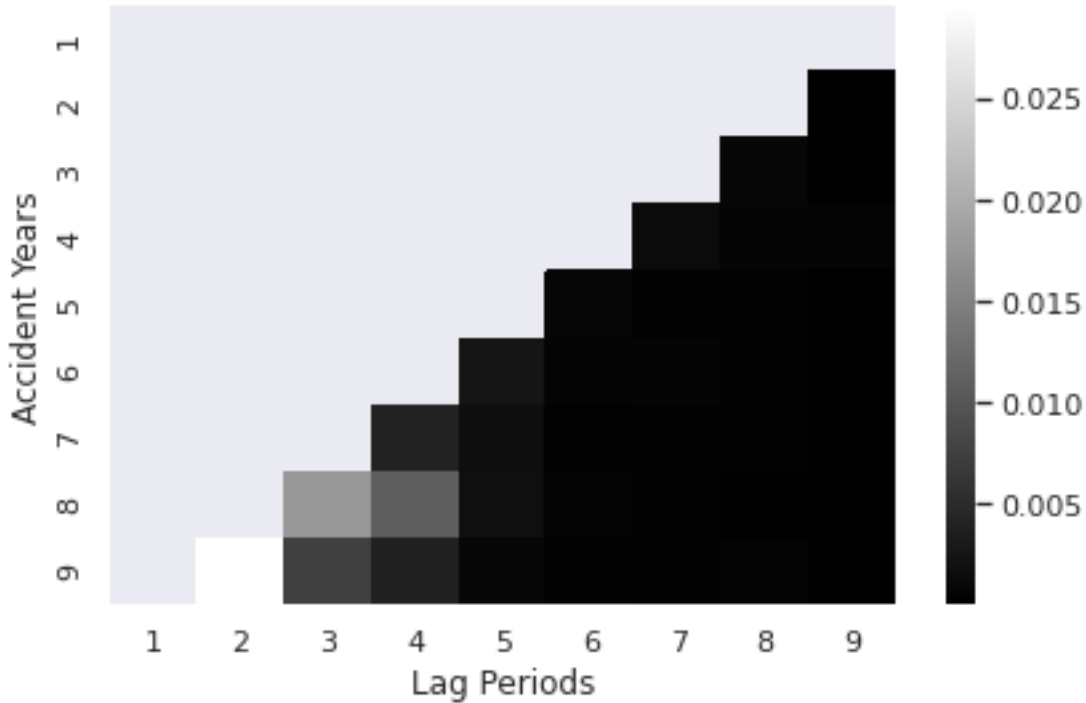
698

699

Figure 19: How the entropy analysis works

700 Figure 20 shows the resulting entropy plot. As anticipated, the earlier lags of
 701 later accident years show the most entropy, with a lighter shade showing higher
 702 values (lower is better). It should also be noted that the later loss development
 703 factors of any accident year are lower in entropy, affirming the inferences made
 704 about the nature of the overall model. One plausible reason for this flaw of the
 705 overall model may be the limiting characteristics of using a single sequence. Ide-
 706 ally, a second sequence may be able to enable the learning of more patterns. The

707 predicted performances deteriorate for the later accident years and from this plot,
708 we can infer that most of the deterioration occurs at the earlier lag periods and
709 that this error is propagated to the later lag periods as well.



710

711

Figure 20: Entropy analysis for the whole model

712 10.2 Discussion

713 This project was undertaken with the aim of exploring the possibilities of applica-
714 tions of deep learning in the field of actuarial science. Whilst deep learning may
715 not be as popular in comparison to the more conventional actuarial methods of
716 analysis, there is little doubt of the impact it is due to make in the coming years,
717 especially considering that explosion of the diversity and the vastness of the data
718 that will become ripe for analytics in the future. This project is a minute attempt
719 to contend with a fundamental actuarial problem, in the vast backdrop of the daz-
720 zling field of deep learning.

721 The biggest challenge faced in the context of implementing this project was
722 finding good data that is representative of the real world data. Within this project,
723 data from CAS was used. The nature of deep learning is such that it requires fairly
724 large amounts of data. If larger data sets of comparable type were found, there

725 is more than a fair chance that the predictions could have been of much more
726 superior accuracy.

727 Another aspect that needs to be highlighted here is the ability of deep learning
728 algorithms to require minimal expert user input. However, this does not mean
729 that we can transcend the limitations of pattern recognition imposed by funda-
730 mental laws/theorems of statistics. A case and point of this is how and why we
731 had to normalize loss sequences in a certain manner. The fact that only cumula-
732 tive paid losses were used also imposed restrictions on the predictive power, since
733 each accident year had only a single channel of a pattern sequence.

734 Despite these limitations, other than the choice of how to normalize the data
735 as loss development factors, almost all other decisions were related to program-
736 ming/fundamentals of data science and statistics. The next possible frontier of
737 this project would be the collection of diverse traditional and nontraditional data
738 pertaining to loss reserving, into a single data set, and then building a model that
739 can predict ultimate losses using this diverse portfolio of data.

740 References

- 741 [1] Alzubaidi, L., Zhang, J., Humaidi, A. J., Al-Dujaili, A., Duan, Y., Al-Shamma,
742 O., Santamaría, J., Fadhel, M. A., Al-Amidie, M., & Farhan, L. (2021, March
743 31). Review of deep learning: concepts, CNN architectures, challenges, ap-
744 plications, future directions. *Journal of Big Data*, 20. [https://doi.org/10.](https://doi.org/10.1186/s40537-021-00444-8)
745 [1186/s40537-021-00444-8](https://doi.org/10.1186/s40537-021-00444-8)
- 746 [2] Amin, Z., Antonio, K., Beirlant, J., Charpentier, A., Dean, C. G., Frees, E.
747 W., Gan, G., Gao, L., Garrido, J., Hua, L., Ismail, N., Kim, J. H., Okine,
748 N.-A., Sarıdaş, E. S., Shi, P., Shyamalkumar, N. D., Su, J., Verdonck, T., &
749 Viswanathan, K. (2020, August 23). *Loss Data Analytics*. Chapter 11 Loss
750 Reserving. Retrieved September 25, 2021, from [https://openacttexts.](https://openacttexts.github.io/Loss-Data-Analytics/C-LossReserves.html)
751 [github.io/Loss-Data-Analytics/C-LossReserves.html](https://openacttexts.github.io/Loss-Data-Analytics/C-LossReserves.html)
- 752 [3] Baier, L., Hofmann, M., Kühl, N., Mohr, M., & Satzger, G. (2020, April 1).
753 *Handling Concept Drifts in Regression Problems - the Error Intersection Ap-*
754 *proach*. arxiv. Retrieved October 31, 2021, from [https://arxiv.org/abs/](https://arxiv.org/abs/2004.00438)
755 [2004.00438\#](https://arxiv.org/abs/2004.00438)

- 756 [4] Basaldella, M., Antolli, E., Serra, G., & Tasso, C. (2018). Bidirectional LSTM
757 Recurrent Neural Network for Keyphrase Extraction. In *Digital Libraries*
758 *and Multimedia Archive* (182, 183). Springer. [https://link.springer.com/
759 book/10.1007/978-3-319-73165-0](https://link.springer.com/book/10.1007/978-3-319-73165-0)
- 760 [5] *Chain Ladder - Reserving in Python*. (2021). Welcome to Chainlad-
761 der. Retrieved October 10, 2021, from [https://chainladder-python.
762 readthedocs.io/en/latest/intro.html](https://chainladder-python.readthedocs.io/en/latest/intro.html)
- 763 [6] Chollet, F. (2018). *Deep Learning with Python*. Manning Publications.
764 [https://learning.oreilly.com/library/view/deep-learning-
765 with/9781617294433/OEBPS/Text/title.xhtml](https://learning.oreilly.com/library/view/deep-learning-with/9781617294433/OEBPS/Text/title.xhtml)
- 766 [7] Clark, R. C., & Rangelova, D. (2021). *Accident Year / Development Year*
767 *Interactions*. CAS. [https://www.casact.org/sites/default/files/2021-
768 02/pubs_forum_15fforum_clarkrangelova.pdf](https://www.casact.org/sites/default/files/2021-02/pubs_forum_15fforum_clarkrangelova.pdf)
- 769 [8] de Myttenaere, A., Golden, B., Le Grand, B., & Rossi, F. (2015, June 12). *Us-*
770 *ing the Mean Absolute Percentage Error for Regression Models*. arxiv. Retrieved
771 October 10, 2021, from <https://arxiv.org/abs/1605.02541>
- 772 [9] England, P. D., & Verrral, R. J. (11, June 10). Stochastic Claims Re-
773 serving in General Insurance. *British Actuarial Journal*, 8(3). 10.1017/
774 S1357321700003809
- 775 [10] Feng, J., & Lu, S. (2019). Performance Analysis of Various Activation Func-
776 tions in Artificial Neural Networks. *Journal of Physics: Conference Series Paper*,
777 1237(2) 10.1088/1742-6596/1237/2/022030
- 778 [11] Giles, C. L., Lawrence, S., & Tsoi, A. C. (2001, July). Noisy Time Series Predic-
779 tion using Recurrent Neural Networks and Grammatical Inference. *Machine*
780 *Learning*, (44), 161–183. <https://doi.org/10.1023/A:1010884214864>
- 781 [12] Google. (2021, August 27). *Machine Learning Glossary*. Machine Learning
782 Glossary. Retrieved October 30, 2021, from [https://developers.google.
783 com/machine-learning/glossary/#embeddings](https://developers.google.com/machine-learning/glossary/#embeddings)
- 784 [13] Harej, B., Gächter, R., & Jamal, S. (2017). *Individual Claim Development with*
785 *Machine Learning* [2017 Report by Austin]. Austin.

- 786 [14] Hastie, T., Tibshirani, R., & Friedman, J. (2017). *The Elements of Statistical*
787 *Learning Data Mining, Inference, and Prediction* (2nd ed.). Springer.
- 788 [15] Meyers, G. G., & Shi, P. (n.d.). *Loss Reserving Data Pulled from*
789 *NAIC Schedule P*. CAS. Retrieved October 28, 2021, from <https://www.casact.org/publications-research/research/research-resources/loss-reserving-data-pulled-naic-schedule-p>
790
791
- 792 [16] Mills, T. C., & Markellos, R. N. (2008). *The Econometric Modelling of Financial*
793 *Time Series* (3rd ed.) Cambridge University Press.
- 794 [17] Nwankpa, C. E., Ijomah, W., Gachagan, A., & Marshall, S. (2018, November
795 8). *Activation Functions: Comparison of Trends in Practice and Research for Deep*
796 *Learning*. Retrieved October 10, 2021, from [https://arxiv.org/abs/1811.](https://arxiv.org/abs/1811.03378)
797 [03378](https://arxiv.org/abs/1811.03378)
- 798 [18] Pascanu, R., Mikolov, T., & Bengio, Y. (2012). Understanding the exploding
799 gradient problem. *CoRR*, *abs/1211.5063*. Retrieved October 10, 2021, from
800 <http://arxiv.org/abs/1211.5063>
- 801 [19] Radtke, M. (2016). Run-Off Data. In *Handbook on Loss Reserving* (pp. 241-
802 245). Springer. 10.1007/978-3-319-30056-6_32
- 803 [20] Radtke, M. (2016). Separation Method. In *Handbook on Loss Reserving* (pp.
804 247-254). Springer. 10.1007/978-3-319-30056-6_33
- 805 [21] Ramsay, C. M. (2007). New method of estimating loss reserves. In *Proceedings*
806 *of the Casualty Actuarial Society* (Vol. 92, pp. 462-485). Casualty Actuarial
807 Society.
- 808 [22] Richman, R. (2020, August 26). AI in actuarial science – a review of recent
809 advances – part 1. *Annals of Actuarial Science*, *15*(2), 230 - 258. [https://doi.](https://doi.org/10.1017/S1748499520000238)
810 [org/10.1017/S1748499520000238](https://doi.org/10.1017/S1748499520000238)
- 811 [23] Sánchez-Sánchez, P. A., García-González, J. R., & Coronell, L. H. (2019). En-
812 countered Problems of Time Series with Neural Networks: Models and Archi-
813 tectures - Difficulties in the prediction of time series with neural networks. In
814 *Recent Trends in Artificial Neural Networks - from Training to Prediction*. Intech
815 Open. 10.5772/intechopen.88901

- 816 [24] Schmidt, K. D. (2016). Run-Off Triangles. In *Handbook on Loss Reserving* (pp.
817 245-263). Springer. 10.1007/978-3-319-30056-6_34
- 818 [25] Sherstinsky, A. (2020). Fundamentals of Recurrent Neural Network (RNN)
819 and Long Short-Term Memory (LSTM) network. *Physica D: Nonlinear Phenom-*
820 *ena*, 404(3), 1. doi.org/10.1016/j.physd.2019.132306
- 821 [26] Suliman, A., & Zhang, Y. (2015, January 25). A Review on Back-Propagation
822 Neural Networks in the Application of Remote Sensing Image Classification.
823 *Journal of Earth Science and Engineering*, 5. 10.17265/2159-581X/2015.01.
824 004
- 825 [27] Sutton, R. S., & Barto, A. G. (2018). *Reinforcement Learning: An Introduction*
826 (Second ed.). The MIT Press.
- 827 [28] Zhang, A., Lipton, Z. C., Li, M., & Smola, A. J. (2021). Linear Neural Network.
828 In *Dive into Deep Learning*. [https://d21.ai/chapter_linear-networks/
829 index.html](https://d21.ai/chapter_linear-networks/index.html)
- 830 [29] Zhang, A., Lipton, Z. C., Li, M., Smola, A. J., Werness, B., Hu, R., Zhang,
831 S., Tay, Y., Dagar, A., & Tang, Y. (2021). Recurrent Neural Networks.
832 In *Dive into Deep Learning*. [https://d21.ai/chapter_recurrent-neural-
833 networks/index.html](https://d21.ai/chapter_recurrent-neural-networks/index.html)